

Vacuum polarization in a one-dimensional effective quantum-electrodynamics model

Timothée Audinet,^{1,*} Umberto Morellini,^{2,1,†} Antoine Levitt,^{3,‡} and Julien Toulouse^{1,4,§}

¹*Laboratoire de Chimie Théorique, Sorbonne Université and CNRS, F-75005 Paris, France*

²*CEREMADE, Université Paris-Dauphine-PSL and CNRS, F-75016 Paris, France*

³*Laboratoire de mathématiques d'Orsay, Université Paris-Saclay and CNRS, F-91405 Orsay, France*

⁴*Institut Universitaire de France, F-75005 Paris, France*

(Dated: October 24, 2024)

With the aim of progressing toward a practical implementation of an effective quantum-electrodynamics (QED) theory of atoms and molecules, which includes the effects of vacuum polarization through the creation of virtual electron-positron pairs but without the explicit photon degrees of freedom, we study a one-dimensional effective QED model of the hydrogen-like atom with delta-potential interactions. This model resembles the three-dimensional effective QED theory with Coulomb interactions while being substantially simpler. We provide some mathematical details about the definition of this model, calculate the vacuum-polarization density, and the Lamb-type shift of the bound-state energy, correcting and extending results of previous works. We also study the approximation of the model in a finite plane-wave basis, and in particular we discuss the basis convergence of the bound-state energy and eigenfunction, of the vacuum-polarization density, and of the Lamb-type shift of the bound-state energy. We highlight the difficulty of converging the vacuum-polarization density in a finite basis and we propose a way to improve it. The present work could give hints on how to perform similar calculations for the three-dimensional effective QED theory of atoms and molecules.

* timothee.audinet@sorbonne-universite.fr

† morellini@ceremade.dauphine.fr

‡ antoine.levitt@universite-paris-saclay.fr

§ toulouse@lct.jussieu.fr

I. INTRODUCTION

It is important to take into account the effects of special relativity in the quantum electronic-structure theory of atoms, molecules, and solids [1–3]. State-of-the-art relativistic electronic-structure calculations are based on the Dirac-Coulomb-Breit Hamiltonian in the no-pair approximation (see, e.g., Refs. 4–6). The next step is to go beyond the no-pair approximation, i.e. including the quantum-electrodynamics (QED) effect of virtual electron-positron pairs. This is not only important for highly accurate calculations, but also to put relativistic electronic-structure theory on deeper theoretical grounds.

Highly accurate bound-state QED perturbative methods have been developed but are limited to few-electron atomic systems (see, e.g., Refs. 7–11). For many-electron atoms and molecules, it has been proposed to estimate QED corrections with model one-electron operators (see, e.g., Refs. 12–21). An appealing approach for ab initio relativistic electronic-structure calculations beyond the no-pair approximation is given by an effective QED theory, which includes the effects of vacuum polarization through the creation of virtual electron-positron pairs but still uses a static Coulomb or Coulomb-Breit two-particle interaction instead of explicit photons (see, e.g., Refs. [4, 22–30]). This effective QED theory with the Coulomb two-particle interaction has been the subject of a number of detailed mathematical studies which established the soundness of this approach at the Hartree-Fock level [31–38]. Based on this effective QED theory, it has been proposed to formulate a relativistic density-functional theory [28] and a relativistic reduced density-matrix functional theory [39].

As in full QED, the difficulty with this effective QED theory lies in the fact that it contains infinities. In particular, the vacuum-polarization density diverges in the ultraviolet (UV) limit (see, e.g., Ref. 40). This UV divergence can be regularized with a UV momentum cutoff and the dependence on the cutoff can be absorbed into a redefinition of the elementary charge, which is called charge renormalization (see, e.g., Refs. 34 and 38). However, it is presently not clear how to deal with this situation in a finite basis and consequently no practical implementation of this effective QED theory has been done so far.

To progress toward the goal of a practical implementation of the above-mentioned effective QED theory for atomic and molecular calculations, this theory was studied in Ref. 30 in the context of a one-dimensional (1D) model of the relativistic hydrogen-like atom using delta-potential interactions. In the non-relativistic version of this model [41–44], the use of the delta potential is motivated by the fact that it leads to the same ground-state energy and wave function as the ground-state energy and radial wave function of the three-dimensional (3D) hydrogen-like atom with the Coulomb potential. The relativistic version of this model without QED effects was also previously studied [45–48]. The calculation of the vacuum-polarization density in this model was first attempted in Ref. 49. A more thorough study of the QED effects, including the Lamb-type shift of the bound-state energy, was performed in Ref. 30. The interest in this 1D effective QED model lies in the fact that it resembles the 3D effective QED theory with Coulomb interactions while being substantially simpler.

In the present work, we reexamine in more mathematical details this 1D effective QED model, correcting and extending results of previous works. In particular, we perform a more careful calculation of the exact vacuum-polarization density and show that there is a Dirac-delta contribution that was missed in the previous calculations. We also study the calculation of the vacuum-polarization density in a finite plane-wave basis, highlighting the difficulty of converging this quantity with the size of the basis, and we propose a way to improve the convergence of the calculation.

The paper is organized as follows. In Section II, we provide the mathematical definition of the 1D hydrogen-like Dirac model, we perform the calculation of the exact vacuum-polarization density, and discuss the resulting QED correction to the bound-state energy. In Section III, we study the approximation of the model in a finite plane-wave basis: we discuss the convergence of the bound-state energy and eigenfunction, the convergence of the vacuum-polarization density, and the convergence of the QED correction to the bound-state energy with respect to the size of the basis. Finally, Section IV contains our conclusions. In the appendices, we provide some mathematical details about the definition of the Hamiltonian of the present model and about the rate of convergence of the bound-state energy in a plane-wave basis.

II. EXACT 1D HYDROGEN-LIKE DIRAC MODEL

In this section, we study the exact 1D hydrogen-like Dirac model in the infinite-dimensional setting.

A. Hamiltonian

We consider a 1D spinless relativistic electron with two-component states in the Hilbert space $\mathfrak{h} = L^2(\mathbb{R}, \mathbb{C}^2)$. The 1D hydrogen-like Dirac Hamiltonian with an electrostatic-type nucleus-electron Dirac-delta potential can be formally

defined as [30, 46]

$$\mathbf{D}_Z = \mathbf{D}_0 - Z\delta(x)\mathbf{I}_2, \quad (1)$$

where \mathbf{D}_0 is the 1D free 2×2 Dirac Hamiltonian

$$\mathbf{D}_0 = c\boldsymbol{\sigma}_1 p_x + \boldsymbol{\sigma}_3 mc^2, \quad (2)$$

where $p_x = -i\partial/dx$ is the momentum operator, c is the speed of light, m is the electron mass, and $\boldsymbol{\sigma}_1$ and $\boldsymbol{\sigma}_3$ are the 2×2 Pauli matrices

$$\boldsymbol{\sigma}_1 = \begin{pmatrix} 0 & 1 \\ 1 & 0 \end{pmatrix} \quad \text{and} \quad \boldsymbol{\sigma}_3 = \begin{pmatrix} 1 & 0 \\ 0 & -1 \end{pmatrix}, \quad (3)$$

and $Z \geq 0$ is the nuclear charge and \mathbf{I}_2 is the 2×2 identity matrix. For all the other usual physical constants, we always assume atomic units in which $\hbar = e = 4\pi\epsilon_0 = 1$.

The delta potential in Eq. (1) makes in fact the definition of \mathbf{D}_Z ambiguous. There are several self-adjoint operators \mathbf{D}_Z compatible with the above formal definition. As in Ref. 30, we choose the self-adjoint operator \mathbf{D}_Z defined as having the same action of \mathbf{D}_0 for $x \neq 0$, i.e.

$$\mathbf{D}_Z\psi = \mathbf{D}_0\psi \quad \text{on } \mathbb{R} \setminus \{0\}, \quad (4)$$

with the Z -dependent domain [50–54]

$$\text{Dom}(\mathbf{D}_Z) = \{\psi \in H^1(\mathbb{R} \setminus \{0\}, \mathbb{C}^2) \mid \psi(0^+) = \mathbf{M}_Z\psi(0^-)\}. \quad (5)$$

In Eq. (5), $H^1(\mathbb{R} \setminus \{0\}, \mathbb{C}^2) \equiv H^1(\mathbb{R}^-, \mathbb{C}^2) \oplus H^1(\mathbb{R}^+, \mathbb{C}^2)$ is the first-order broken Sobolev space (allowing for a non-square-integrable derivative only at $x = 0$) expressed with the standard first-order Sobolev space $H^1(\Omega, \mathbb{C}^2) = \{\psi \in L^2(\Omega, \mathbb{C}^2) \mid d\psi/dx \in L^2(\Omega, \mathbb{C}^2)\}$ for a domain $\Omega \subseteq \mathbb{R}$, and \mathbf{M}_Z is the following unitary 2×2 matrix enforcing a boundary condition at $x = 0$ [45–47]

$$\mathbf{M}_Z = \begin{pmatrix} \cos\theta & i\sin\theta \\ i\sin\theta & \cos\theta \end{pmatrix}, \quad (6)$$

with $\theta = 2\arctan(Z/2c)$.

The Hamiltonian \mathbf{D}_Z has a single bound state with energy [30, 46, 49, 55]

$$\varepsilon_b^Z = mc^2 \frac{1 - (Z/2c)^2}{1 + (Z/2c)^2}, \quad (7)$$

and eigenfunction

$$\psi_b^Z(x) = A_b \begin{pmatrix} 1 \\ i\text{sgn}(x)Z/2c \end{pmatrix} e^{-\kappa_b|x|}, \quad (8)$$

where sgn is the sign function, $\kappa_b = mZ/(1 + (Z/2c)^2)$, and $A_b = \sqrt{\kappa_b/(1 + (Z/2c)^2)}$. Note that the large (upper) component of the bound-state eigenfunction is an even function of x , while the small (lower) component is an odd function of x with a discontinuity at $x = 0$. Beside the eigenvalue ε_b^Z , the Hamiltonian \mathbf{D}_Z has also a continuous energy spectrum $(-\infty, -mc^2] \cup [mc^2, +\infty)$. At $Z = 0$, only the continuous energy spectrum $(-\infty, -mc^2] \cup [mc^2, +\infty)$ remains. The bound-state energy in Eq. (7) is strictly positive for $Z < 2c$. Moreover, the bound-state energy level never dives into the negative-energy continuum for all $Z > 0$. The bound-state energy only approaches the top of the negative-energy continuum as $Z \rightarrow \infty$, i.e. $\lim_{Z \rightarrow \infty} \varepsilon_b^Z = -mc^2$. Hence, there are no supercritical QED effects in the present model [56, 57].

In Appendix A, we argue that the matrix elements of the Hamiltonian \mathbf{D}_Z can be defined on a larger Z -independent set of functions with the expression

$$\langle \phi, \mathbf{D}_Z\psi \rangle = \langle \phi, \mathbf{D}_0\psi \rangle - Z\bar{\phi}^\dagger(0)\bar{\psi}(0), \quad (9)$$

where $\langle \cdot, \cdot \rangle$ designates the inner product of $L^2(\mathbb{R}, \mathbb{C}^2)$, and $\bar{\psi}(0) = [\psi(0^+) + \psi(0^-)]/2$ and $\bar{\phi}(0) = [\phi(0^+) + \phi(0^-)]/2$. Importantly, Eq. (9) can be used to calculate the matrix elements of the Hamiltonian on a basis of functions which are continuous and thus which do not belong to the domain considered in Eq. (5).

B. Vacuum-polarization density

The vacuum-polarization density $n^{\text{VP}}(x)$ for the 1D hydrogen-like Dirac model was calculated in Refs. 30 and 49. However, these calculations were only valid for $x \neq 0$. Here, we reexamine the calculation of the vacuum-polarization density using the momentum-space Green function and show that there is a Dirac-delta function contribution at $x = 0$ that was missed in the previously cited works. In order to make things mathematically simpler, we will now work on the following Hilbert space with a UV momentum cutoff parameter Λ (similarly to the 3D case, see e.g. Ref. 34)

$$\mathfrak{h}_\Lambda = \left\{ \boldsymbol{\psi} \in \mathfrak{h} \mid \hat{\boldsymbol{\psi}}(p) = \mathbf{0} \text{ for } |p| > \Lambda \right\}, \quad (10)$$

where $\hat{\boldsymbol{\psi}}$ is the Fourier transform of $\boldsymbol{\psi}$. We will then be interested in the infinite UV momentum cutoff limit, i.e. $\Lambda \rightarrow \infty$.

1. General expression in terms of the Green function

The formal definition of the Hamiltonian in Eq. (1) or the definition via matrix elements in Eq. (9) leads to the following expression for the 1D hydrogen-like Dirac Hamiltonian in momentum space (for $|p| \leq \Lambda$ and $|p'| \leq \Lambda$)

$$\mathbf{D}_Z(p, p') = \mathbf{D}_0(p, p') + \mathbf{V}(p, p'), \quad (11)$$

with

$$\mathbf{D}_0(p, p') = \delta(p - p') [c\boldsymbol{\sigma}_1 p + \boldsymbol{\sigma}_3 m c^2] \text{ and } \mathbf{V}(p, p') = -\frac{Z}{2\pi} \mathbf{I}_2. \quad (12)$$

The Green function (or resolvent) operator $\mathbf{G}_0(\omega) = (\omega \mathbf{I}_2 - \mathbf{D}_0)^{-1}$ of the 1D free Dirac Hamiltonian \mathbf{D}_0 in momentum space is, for $\omega \in \mathbb{C} \setminus \sigma(\mathbf{D}_0)$ where $\sigma(\mathbf{D}_0)$ is the spectrum of \mathbf{D}_0 ,

$$\mathbf{G}_0(p, p'; \omega) = \frac{\delta(p - p')}{\omega^2 - \varepsilon_p^2} \begin{pmatrix} mc^2 + \omega & cp \\ cp & -mc^2 + \omega \end{pmatrix}, \quad (13)$$

with $\varepsilon_p = \sqrt{p^2 c^2 + m^2 c^4}$. The Green function operator $\mathbf{G}_Z(\omega) = (\omega \mathbf{I}_2 - \mathbf{D}_Z)^{-1}$ of the 1D hydrogen-like Dirac Hamiltonian \mathbf{D}_Z in momentum space satisfies the Dyson equation, for $\omega \in \mathbb{C} \setminus \sigma(\mathbf{D}_Z)$,

$$\mathbf{G}_Z(p, p'; \omega) = \mathbf{G}_0(p, p'; \omega) + \int_{-\Lambda}^{\Lambda} \int_{-\Lambda}^{\Lambda} \mathbf{G}_0(p, p_1; \omega) \mathbf{V}(p_1, p_2) \mathbf{G}_Z(p_2, p'; \omega) dp_1 dp_2. \quad (14)$$

Using the expression of $\mathbf{V}(p, p')$, the Dyson equation can be simplified as

$$\mathbf{G}_Z(p, p'; \omega) = \mathbf{G}_0(p, p'; \omega) - \frac{Z}{2\pi} \bar{\mathbf{G}}_0(p; \omega) \bar{\mathbf{G}}_Z(p'; \omega), \quad (15)$$

where $\bar{\mathbf{G}}_0(p, \omega) = \int_{-\Lambda}^{\Lambda} \mathbf{G}_0(p, p_1; \omega) dp_1$ and $\bar{\mathbf{G}}_Z(p'; \omega) = \int_{-\Lambda}^{\Lambda} \mathbf{G}_Z(p_2, p'; \omega) dp_2$. Integrating Eq. (15) over p gives

$$\bar{\mathbf{G}}_Z(p'; \omega) = \bar{\mathbf{G}}_0(p'; \omega) - \frac{Z}{2\pi} \bar{\bar{\mathbf{G}}}_0(\omega) \bar{\mathbf{G}}_Z(p'; \omega), \quad (16)$$

where $\bar{\bar{\mathbf{G}}}_0(\omega) = \int_{-\Lambda}^{\Lambda} \bar{\mathbf{G}}_0(p; \omega) dp$, and thus

$$\bar{\mathbf{G}}_Z(p'; \omega) = \left[\mathbf{I}_2 + \frac{Z}{2\pi} \bar{\bar{\mathbf{G}}}_0(\omega) \right]^{-1} \bar{\mathbf{G}}_0(p'; \omega). \quad (17)$$

Inserting the last expression in Eq. (15), we obtain for the variation of the Green function due to the nucleus-electron potential, $\Delta \mathbf{G}_Z(p, p'; \omega) = \mathbf{G}_Z(p, p'; \omega) - \mathbf{G}_0(p, p'; \omega)$,

$$\Delta \mathbf{G}_Z(p, p'; \omega) = -\frac{Z}{2\pi} \bar{\mathbf{G}}_0(p; \omega) \left[\mathbf{I}_2 + \frac{Z}{2\pi} \bar{\bar{\mathbf{G}}}_0(\omega) \right]^{-1} \bar{\mathbf{G}}_0(p'; \omega). \quad (18)$$

From Eq. (13), we can calculate $\bar{\mathbf{G}}_0(p; \omega)$ and $\bar{\mathbf{G}}_0(\omega)$,

$$\bar{\mathbf{G}}_0(p; \omega) = \frac{1}{\omega^2 - \varepsilon_p^2} \begin{pmatrix} mc^2 + \omega & cp \\ cp & -mc^2 + \omega \end{pmatrix}, \quad (19)$$

and

$$\bar{\mathbf{G}}_0(\omega) = \frac{\pi \xi(\Lambda, \omega)}{c} \begin{pmatrix} -g(\omega) & 0 \\ 0 & g(-\omega) \end{pmatrix}, \quad (20)$$

with $g(\omega) = \sqrt{(mc^2 + \omega)/(mc^2 - \omega)}$ and $\xi(\Lambda, \omega) = (2/\pi) \arctan(c\Lambda/\sqrt{m^2c^4 - \omega^2})$. Note that the function $\xi(\Lambda, \omega)$ reduces to 1 in the infinite UV momentum cutoff limit, i.e. $\lim_{\Lambda \rightarrow \infty} \xi(\Lambda, \omega) = 1$. Note also that the zero off-diagonal elements in Eq. (20) come from the fact that we have integrated an odd function of p over the symmetric interval $[-\Lambda, \Lambda]$, i.e. $\int_{-\Lambda}^{\Lambda} cp/(\omega^2 - \varepsilon_p^2) dp = 0$. A non-symmetric UV momentum cutoff gives non-zero off-diagonal elements (see Appendix B). So, the Green function obtained in the limit $\Lambda \rightarrow \infty$ depends on how the UV momentum cutoff is chosen. The symmetric UV momentum cutoff correctly gives, in the limit $\Lambda \rightarrow \infty$, the Green function corresponding to the Hamiltonian defined by Eqs. (4) and (5), which was already calculated in position space using different methods in Refs. 30 and 50. From Eqs. (18)-(20), we finally arrive at the expression of the variation of the Green function in momentum space

$$\Delta \mathbf{G}_Z(p, p'; \omega) = -\frac{Z}{2\pi} \frac{z_1(\omega) \mathbf{A}_1(p, p'; \omega) + z_2(\omega) \mathbf{A}_2(p, p'; \omega)}{(\omega^2 - \varepsilon_p^2)(\omega^2 - \varepsilon_{p'}^2)}, \quad (21)$$

with $z_1(\omega) = (1 - Zg(\omega)\xi(\Lambda, \omega)/2c)^{-1}$ and $z_2(\omega) = (1 + Zg(-\omega)\xi(\Lambda, \omega)/2c)^{-1}$, and $\mathbf{A}_1(p, p'; \omega)$ and $\mathbf{A}_2(p, p'; \omega)$ are the following matrices

$$\mathbf{A}_1(p, p'; \omega) = \begin{pmatrix} (mc^2 + \omega)^2 & cp'(mc^2 + \omega) \\ cp(mc^2 + \omega) & c^2pp' \end{pmatrix} \text{ and } \mathbf{A}_2(p, p'; \omega) = \begin{pmatrix} c^2pp' & cp(-mc^2 + \omega) \\ cp'(-mc^2 + \omega) & (-mc^2 + \omega)^2 \end{pmatrix}. \quad (22)$$

The Fourier transform of the vacuum-polarization density matrix is given by (see, e.g., Refs. 34, 40, 58, and 59)

$$\hat{\mathbf{n}}_1^{\text{VP}}(p, p') = \frac{1}{2\pi} \int_{-\infty}^{\infty} \Delta \mathbf{G}_Z(p, p'; iu + \gamma) du, \quad (23)$$

where γ is a real constant such that $-mc^2 < \gamma < \varepsilon_b^Z$, and the Fourier transform of the local vacuum-polarization density matrix can then be obtained as (see, e.g., Refs. 36, 40, and 60)

$$\hat{\mathbf{n}}_{\Lambda}^{\text{VP}}(k) = \frac{1}{\sqrt{2\pi}} \int_{\substack{|p+k/2| \leq \Lambda \\ |p-k/2| \leq \Lambda}} \hat{\mathbf{n}}_1^{\text{VP}}(p + k/2, p - k/2) dp, \quad (24)$$

where, for clarity, we have explicitly indicated the dependence on the UV momentum cutoff parameter Λ in $\hat{\mathbf{n}}_{\Lambda}^{\text{VP}}(k)$. The constant γ in Eq. (23) is there so that the integration of u selects only the continuous negative-energy spectrum and not the bound-state energy ε_b^Z . From now on, we will assume that $Z < 2c$ so that the bound-state eigenvalue ε_b^Z is always strictly positive, and we will choose $\gamma = 0$. What we call the local vacuum-polarization density matrix is thus obtained as the inverse Fourier transform of $\hat{\mathbf{n}}_{\Lambda}^{\text{VP}}(k)$

$$\mathbf{n}_{\Lambda}^{\text{VP}}(x) = \frac{1}{\sqrt{2\pi}} \int_{-\infty}^{\infty} \hat{\mathbf{n}}_{\Lambda}^{\text{VP}}(k) e^{ikx} dk, \quad (25)$$

i.e., it is the position-space diagonal of the vacuum-polarization density matrix. Note that the slowest-decaying terms in the integrand in Eq. (23) decay as $1/u^2$, so that the corresponding integral over u is convergent. Note also that, due to the integration domain in Eq. (24), $\hat{\mathbf{n}}_{\Lambda}^{\text{VP}}(k)$ is zero for $|k| > 2\Lambda$. Hence, the integral in Eq. (25) is convergent.

We will see below that, in the limit $\Lambda \rightarrow \infty$, the Fourier transform $\hat{\mathbf{n}}_{\Lambda}^{\text{VP}}(k)$ in Eq. (24) contains terms that go to a constant as $k \rightarrow \pm\infty$ and thus, in this limit, the integral in Eq. (25) contains a Dirac-delta contribution. In fact, in the limit $\Lambda \rightarrow \infty$, the density matrix is not a trace-class operator and defining its associated density is not a priori obvious.

2. Uehling vacuum-polarization density

The integral in Eq. (23) can be analytically calculated at first order in Z , which gives the Fourier transform of the 1D analog of the Uehling vacuum-polarization density matrix

$$\begin{aligned}\hat{\mathbf{n}}_1^{\text{vp},(1)}(p, p') &= \frac{1}{2\pi} \int_{-\infty}^{\infty} \Delta \mathbf{G}_Z^{(1)}(p, p'; iu) du \\ &= -\frac{Z}{4\pi(\varepsilon_p^2 \varepsilon_{p'} + \varepsilon_p \varepsilon_{p'}^2)} \begin{pmatrix} m^2 c^4 + c^2 p p' - \varepsilon_p \varepsilon_{p'} & -m c^3 (p - p') \\ m c^3 (p - p') & m^2 c^4 + c^2 p p' - \varepsilon_p \varepsilon_{p'} \end{pmatrix},\end{aligned}\quad (26)$$

which is independent of Λ , and the Fourier transform of the local Uehling vacuum-polarization density matrix is then obtained using Eq. (24)

$$\hat{\mathbf{n}}_\Lambda^{\text{vp},(1)}(k) = \frac{1}{\sqrt{2\pi}} \int_{\substack{|p+k/2| \leq \Lambda \\ |p-k/2| \leq \Lambda}} \hat{\mathbf{n}}_1^{\text{vp},(1)}(p + k/2, p - k/2) dp. \quad (27)$$

The expression of $\hat{\mathbf{n}}_\Lambda^{\text{vp},(1)}(k)$ resulting from the integration in Eq. (27) is lengthy, but it has a relatively simple expression in the infinite UV momentum cutoff limit,

$$\hat{\mathbf{n}}^{\text{vp},(1)}(k) = \lim_{\Lambda \rightarrow \infty} \hat{\mathbf{n}}_\Lambda^{\text{vp},(1)}(k) = \frac{Z}{(2\pi)^{3/2} c} \mathbf{I}_2 + \hat{\mathbf{n}}_{\text{reg}}^{\text{vp},(1)}(k), \quad (28)$$

which contains a diagonal constant contribution and a regular contribution which goes to zero as $k \rightarrow \pm\infty$

$$\hat{\mathbf{n}}_{\text{reg}}^{\text{vp},(1)}(k) = -\frac{Zm}{(2\pi)^{3/2} h_k} \begin{pmatrix} \frac{4mc}{k} \operatorname{arctanh}\left(\frac{k}{h_k}\right) & \ln\left(\frac{h_k - k}{h_k + k}\right) \\ -\ln\left(\frac{h_k - k}{h_k + k}\right) & \frac{4mc}{k} \operatorname{arctanh}\left(\frac{k}{h_k}\right) \end{pmatrix}, \quad (29)$$

with $h_k = \sqrt{k^2 + 4m^2 c^2}$. Note that, in contrast with the 3D case (see, e.g., Refs. 34 and 40), here there is no divergence in the infinite UV momentum cutoff limit. Therefore, we will implicitly consider this limit in the rest of Section II. Taking the inverse Fourier transform in Eq. (28), we find the local Uehling vacuum-polarization density matrix in position space (in the distribution sense)

$$\mathbf{n}^{\text{vp},(1)}(x) = \frac{Z}{2\pi c} \delta(x) \mathbf{I}_2 + \mathbf{n}_{\text{reg}}^{\text{vp},(1)}(x), \quad (30)$$

where the regular contribution can be expressed as, for $x \neq 0$, (see Appendix D of Ref. 30)

$$\mathbf{n}_{\text{reg}}^{\text{vp},(1)}(x) = -\frac{Z}{4c^2} \int_{-\infty}^{\infty} \frac{du}{2\pi} e^{-2\kappa(iu)|x|} \begin{pmatrix} g(iu)^2 + 1 & -i \operatorname{sgn}(x)[g(iu) + g(-iu)] \\ i \operatorname{sgn}(x)[g(iu) + g(-iu)] & g(-iu)^2 + 1 \end{pmatrix}, \quad (31)$$

with $\kappa(iu) = \sqrt{m^2 c^4 + u^2}/c$. Finally, the Uehling vacuum-polarization density $n^{\text{vp},(1)}(x) = \operatorname{tr}[\mathbf{n}^{\text{vp},(1)}(x)]$ (where tr designates the trace of a 2×2 matrix) has the expression

$$n^{\text{vp},(1)}(x) = \frac{Z}{\pi c} \delta(x) + n_{\text{reg}}^{\text{vp},(1)}(x), \quad (32)$$

where the regular contribution was obtained in Ref. 30 in the compact form

$$n_{\text{reg}}^{\text{vp},(1)}(x) = -\frac{Zm}{\pi} \int_1^\infty \frac{e^{-2mc|x|t}}{t\sqrt{t^2 - 1}} dt. \quad (33)$$

Note that $n^{\text{vp},(1)}(x)$ represents an opposite charge density (or electron-excess density). The vacuum-polarization charge density is the opposite: $\rho^{\text{vp},(1)}(x) = -n^{\text{vp},(1)}(x)$.

The Dirac-delta contribution in Eq. (32) was missed in Ref. 30, in which the calculation was done entirely in position space. The present calculation which starts in momentum space is better suited to correctly catch the Dirac-delta contribution (see, however, Appendix C for how to find the Dirac-delta contribution in position space). The coefficient

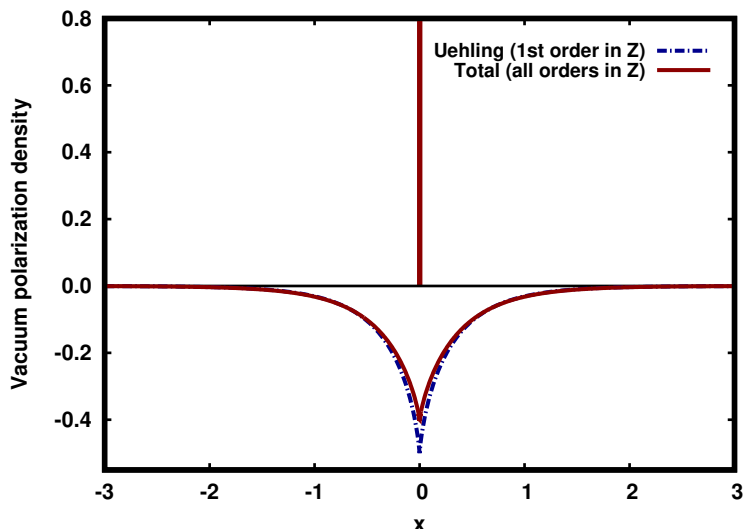


FIG. 1. The Uehling and total vacuum-polarization densities $n^{\text{vp},(1)}(x)$ [Eq. (32)] and $n^{\text{vp}}(x)$ [Eq. (42)] for $m = c = Z = 1$. The vertical line represents a Dirac-delta function.

in front of the Dirac-delta function is exactly the opposite of the spatial integral of the regular contribution $n_{\text{reg}}^{\text{vp},(1)}(x)$, so that the total Uehling vacuum-polarization density integrates to zero, i.e.

$$\int_{-\infty}^{\infty} n^{\text{vp},(1)}(x) dx = 0. \quad (34)$$

The overall shape of the present Uehling vacuum-polarization density, represented in Fig. 1, is consistent with its usual interpretation as the spatial distribution of virtual electron-positron pairs induced by the nuclear charge (see, e.g., Ref. 61), i.e. there is an excess of electrons at the nucleus (the Dirac-delta contribution) and an excess of positrons distributed farther away (the regular contribution).

We emphasize that, in the present 1D model, the Uehling vacuum-polarization density can be obtained without performing any regularization and renormalization. This is in sharp contrast with the case of the 3D hydrogen-like atom for which there is a contribution to the first-order vacuum-polarization density that diverges in momentum space and which is eliminated by charge renormalization. The Uehling vacuum-polarization density is then only the remaining contribution after renormalization (see, e.g., Refs. 40 and 62). This remaining 3D Uehling vacuum-polarization density integrates to zero [59, 62], as in the present 1D model. However, in the 3D hydrogen-like atom, the Uehling vacuum-polarization density (after charge renormalization) has a shape which is the opposite of the one obtained in the present 1D model, i.e. there is an excess of positrons at the nucleus and an excess of electrons farther away [62]. This shape of the Uehling vacuum-polarization density in the 3D hydrogen-like atom may seem counterintuitive but one has to keep in mind that it comes after charge renormalization which has eliminated an (infinite) excess of electrons at the nucleus.

3. Total vacuum-polarization density

The case of the total vacuum-polarization density (i.e., at all orders in Z) is more complicated to study since we have not managed to analytically perform the integral in Eq. (23). Nevertheless, by a mixed analytical-numerical study, we have been able to determine that the Fourier transform of the total vacuum-polarization density matrix has the form (still in the infinite UV momentum cutoff limit)

$$\hat{\mathbf{n}}^{\text{vp}}(k) = \frac{\mathcal{N}_0^{\text{vp}}}{2\sqrt{2\pi}} \mathbf{I}_2 + \hat{\mathbf{n}}_{\text{reg}}^{\text{vp}}(k), \quad (35)$$

with a diagonal constant contribution involving the quantity

$$\mathcal{N}_0^{\text{vp}} = \frac{Z/c}{\pi(1 + (Z/2c)^2)}, \quad (36)$$

and a regular contribution (which goes to zero as $k \rightarrow \pm\infty$) which, in practice, can be obtained by inverting the orders of the integrals in Eqs. (23) and (24), leading to

$$\hat{\mathbf{n}}_{\text{reg}}^{\text{VP}}(k) = -\frac{Z}{\sqrt{2\pi c^2}} \int_{-\infty}^{\infty} \frac{du}{2\pi} \frac{z_1(iu)\mathbf{B}_1(k, u) + z_2(iu)\mathbf{B}_2(k, u)}{\kappa(iu)(k^2 c^2 + 4m^2 c^4 + 4u^2)}, \quad (37)$$

with the matrices

$$\mathbf{B}_1(k, u) = \begin{pmatrix} (mc^2 + iu)^2 & -kc(mc^2 + iu)/2 \\ kc(mc^2 + iu)/2 & m^2 c^4 + u^2 \end{pmatrix} \text{ and } \mathbf{B}_2(k, u) = \begin{pmatrix} m^2 c^4 + u^2 & -kc(mc^2 - iu)/2 \\ kc(mc^2 - iu)/2 & (mc^2 - iu)^2 \end{pmatrix}. \quad (38)$$

In position space, the total vacuum-polarization density matrix is

$$\mathbf{n}^{\text{VP}}(x) = \frac{\mathcal{N}_0^{\text{VP}}}{2} \delta(x) \mathbf{I}_2 + \mathbf{n}_{\text{reg}}^{\text{VP}}(x), \quad (39)$$

where the regular contribution can be expressed as, for $x \neq 0$, (see Appendix D of Ref. 30) [63]

$$\mathbf{n}_{\text{reg}}^{\text{VP}}(x) = -\frac{Z}{4c^2} \int_{-\infty}^{\infty} \frac{du}{2\pi} e^{-2\kappa(iu)|x|} [z_1(iu)\mathbf{C}_1(x, u) + z_2(iu)\mathbf{C}_2(x, u)], \quad (40)$$

with the matrices

$$\mathbf{C}_1(x, u) = \begin{pmatrix} g(iu)^2 & -i \operatorname{sgn}(x)g(iu) \\ i \operatorname{sgn}(x)g(iu) & 1 \end{pmatrix} \text{ and } \mathbf{C}_2(x, u) = \begin{pmatrix} 1 & -i \operatorname{sgn}(x)g(-iu) \\ i \operatorname{sgn}(x)g(-iu) & g(-iu)^2 \end{pmatrix}. \quad (41)$$

Finally, the total vacuum-polarization density $n^{\text{VP}}(x) = \operatorname{tr}[\mathbf{n}^{\text{VP}}(x)]$ has the form

$$n^{\text{VP}}(x) = \mathcal{N}_0^{\text{VP}} \delta(x) + n_{\text{reg}}^{\text{VP}}(x), \quad (42)$$

where the regular part $n_{\text{reg}}^{\text{VP}}(x) = \operatorname{tr}[\mathbf{n}_{\text{reg}}^{\text{VP}}(x)]$ was given in different forms in Refs. 30 and 49. Again, the reason why the Dirac-delta contribution was missed in Refs. 30 and 49 is that these references focused on pointwise calculations of the vacuum-polarization density in position space. The present momentum-space approach avoids this limitation.

The form of the total vacuum-polarization density is very similar to the one of the Uehling vacuum-polarization density, as shown in Fig. 1. However, an important difference is that, for $Z \neq 0$, the total vacuum-polarization density does not integrate to zero

$$\mathcal{N}^{\text{VP}} = \int_{-\infty}^{\infty} n^{\text{VP}}(x) dx = \mathcal{N}_0^{\text{VP}} + \mathcal{N}_{\text{reg}}^{\text{VP}} \neq 0, \quad (43)$$

where the integral of the regular contribution is [30, 49]

$$\mathcal{N}_{\text{reg}}^{\text{VP}} = \int_{-\infty}^{\infty} n_{\text{reg}}^{\text{VP}}(x) dx = -\frac{2}{\pi} \arctan\left(\frac{Z}{2c}\right). \quad (44)$$

We may define the effective nuclear charge observed at a distance d from the nucleus as

$$Z_{\text{obs}}(d) = Z - \int_{-d}^d n^{\text{VP}}(x) dx, \quad (45)$$

with the limits

$$\lim_{d \rightarrow 0^+} Z_{\text{obs}}(d) = Z - \mathcal{N}_0^{\text{VP}} \leq Z, \quad (46)$$

and

$$\lim_{d \rightarrow \infty} Z_{\text{obs}}(d) = Z - \mathcal{N}^{\text{VP}} = Z_{\text{ren}} \geq Z. \quad (47)$$

Thus, at short distances d the vacuum-polarization density screens the nuclear charge, resulting in an observed nuclear charge $Z_{\text{obs}}(d)$ which is smaller than the bare nuclear charge Z . At large distances d from the nucleus ($d \gg \lambda$ where $\lambda = 1/(mc)$ is the reduced Compton wavelength providing a measure of the spatial extension of the vacuum-polarization density), the observed nuclear charge $Z_{\text{obs}}(d)$ is larger than the bare nuclear charge Z . According to the

definition of charge renormalization proposed in Ref. 34, the observed nuclear charge at large distance defines the renormalized nuclear charge Z_{ren} . Thus, in contrast to the case of the 3D hydrogen-like atom, the present 1D model exhibits only a *finite* charge renormalization, without any dependence on the UV momentum cutoff parameter Λ (since we have taken the limit $\Lambda \rightarrow \infty$). Moreover, in the present 1D model the charge renormalization is only due to the vacuum-polarization density beyond the first-order contribution, whereas in the 3D case the charge renormalization is entirely due to the first-order term in the expansion of the vacuum-polarization density in Z . In analogy with the 3D case, the renormalized vacuum-polarization density may be defined as

$$n_{\text{ren}}^{\text{vp}}(x) = -\mathcal{N}_{\text{reg}}^{\text{vp}} \delta(x) + n_{\text{reg}}^{\text{vp}}(x), \quad (48)$$

where the coefficient in front of the delta contribution is chosen so as to make the integral of the renormalized vacuum-polarization density vanish, i.e. $\int_{-\infty}^{\infty} n_{\text{ren}}^{\text{vp}}(x) dx = 0$. Similarly, the renormalized local vacuum-polarization density matrix may be defined as

$$\mathbf{n}_{\text{ren}}^{\text{vp}}(x) = -\frac{\mathcal{N}_{\text{reg}}^{\text{vp}}}{2} \delta(x) \mathbf{I}_2 + \mathbf{n}_{\text{reg}}^{\text{vp}}(x). \quad (49)$$

The finite charge renormalization found in the present model is significantly different from the charge renormalization performed in the 3D case with a finite UV momentum cutoff (see, e.g., Ref. 34). Indeed, we believe that the fact that \mathcal{N}^{vp} is not zero (and not even an integer) in the present model should be understood as an example of fermion-number fractionalization, which is a phenomenon known to appear for 1D Dirac equations with soliton-type potentials (see, e.g., Refs. 64–67). The non-zero value of the fermion number is related to the infrared limit [68–70]. Note, in particular, that the expression of $\mathcal{N}_{\text{reg}}^{\text{vp}}$ in Eq. (44) has the general form of the fermion number found in soliton models [64, 65]. Also, we may note that, in the present model, for $Z = 2c$ the (unoccupied) bound state has zero energy and the spectrum of \mathbf{D}_Z is charge-conjugation symmetric, and $\mathcal{N}_{\text{reg}}^{\text{vp}}$ reduces to $-1/2$, which resembles the soliton scenario of Ref. 71 (see, also, Ref. 67).

In Ref. 30 (Section III.D and Appendix E), it was attempted to calculate the charge of the vacuum of the present model using the notion of “ P^0 -trace” of Refs. 31, 34, and 35. A rough numerical integration suggested that the P^0 -trace formula of the charge of the vacuum gives zero, similarly to what is obtained in the 3D case in the presence of an UV momentum cutoff. However, for the present work, we have performed a more careful numerical integration which shows in fact that the P^0 -trace formula of the (opposite) charge of the vacuum is numerically identical to the integral of the vacuum-polarization density, i.e. the fractional fermion number \mathcal{N}^{vp} . The fact that the P^0 -trace formula of the charge of the vacuum is not an integer implies that the vacuum-polarization density matrix $\hat{\mathbf{n}}_1^{\text{vp}}(p, p')$ [Eq. (23)] of the present model is not a Hilbert-Schmidt operator in the infinite UV momentum cutoff limit (see Refs. 31 and 34). According to the Shale-Stinespring theorem [72, 73], this implies in turn that, in this limit, the polarized vacuum state of the present model cannot be reached from a unitary transformation of the free vacuum state in the second-quantized Fock space (see, also, Refs. 74 and 75).

C. QED corrections to the bound-state energy

In the present 1D hydrogen-like Dirac model, we can calculate the shift of the bound-state energy due to the phenomenon of vacuum polarization, similarly to the Lamb shift in standard QED (see, e.g., Refs. 7 and 19). The analog of the 3D Coulomb-Breit two-particle interaction in the present model is [30, 55]

$$\mathbf{w}(x_1, x_2) = \delta(x_1 - x_2) (\mathbf{I}_2 \otimes \mathbf{I}_2 - \boldsymbol{\sigma}_1 \otimes \boldsymbol{\sigma}_1), \quad (50)$$

where the first and second terms are the 1D analogs of the Coulomb and Breit interactions, respectively (see, e.g., Refs. 5, 6, and 28). Note that, in 1D, the Breit interaction exactly reduces to the magnetic Gaunt interaction [30]. At first order with respect to the two-particle interaction, the QED correction to the bound-state energy contains four contributions [30]

$$\mathcal{E}_b^{\text{vp},(1)} = \mathcal{E}_b^{\text{vp},(1),\text{DC}} + \mathcal{E}_b^{\text{vp},(1),\text{XC}} + \mathcal{E}_b^{\text{vp},(1),\text{DB}} + \mathcal{E}_b^{\text{vp},(1),\text{XB}}. \quad (51)$$

The direct-Coulomb-type (DC) and exchange-Coulomb-type (XC) contributions are

$$\mathcal{E}_b^{\text{vp},(1),\text{DC}} = \int_{-\infty}^{\infty} n^{\text{el}}(x) n_{\text{ren}}^{\text{vp}}(x) dx, \quad (52)$$

and

$$\mathcal{E}_b^{\text{vp},(1),\text{XC}} = - \int_{-\infty}^{\infty} \text{tr}[\mathbf{n}^{\text{el}}(x) \mathbf{n}_{\text{ren}}^{\text{vp}}(x)] dx, \quad (53)$$

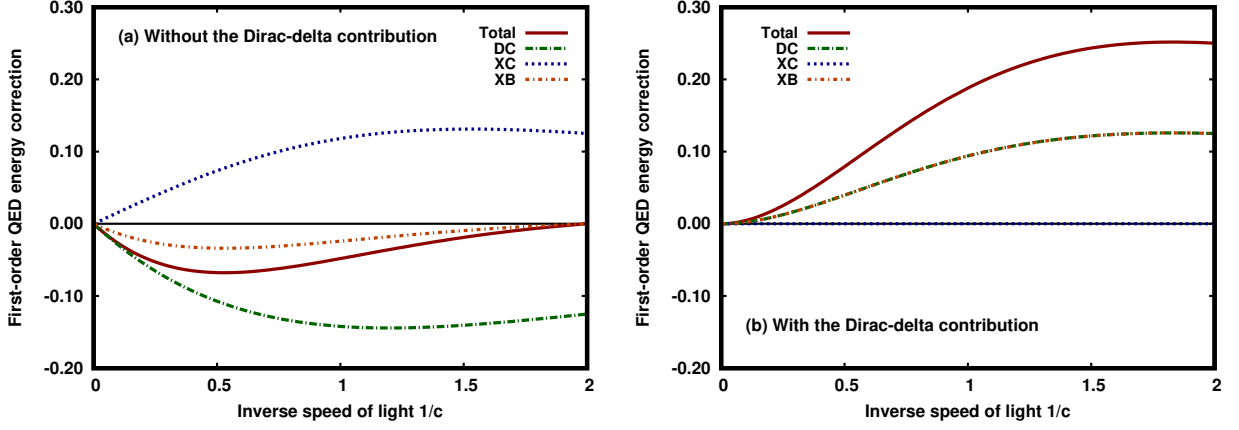


FIG. 2. First-order QED correction to the bound-state energy [Eq. (51)] for $m = Z = 1$ as a function of the inverse speed of light $1/c$, using the renormalized local vacuum-polarization density matrix [Eq. (49)] (a) without the Dirac-delta contribution $-(\mathcal{N}_{\text{reg}}^{\text{vp}}/2)\delta(x)\mathbf{I}_2$ and (b) with the Dirac-delta contribution $-(\mathcal{N}_{\text{reg}}^{\text{vp}}/2)\delta(x)\mathbf{I}_2$. The total correction, as well as the direct-Coulomb-type (DC) [Eq. 52], exchange-Coulomb-type (XC) [Eq. 53], and exchange-Breit-type (XB) [Eq. 55] contributions are shown. On plot (a), the curve DC is identical to the one in Fig. 3 of Ref. 30 but the curves XC and XB are different since there was an error in the off-diagonal elements of the expression of $\mathbf{n}_{\text{reg}}^{\text{vp}}(x)$ given in Ref. 30, as explained in the note [63].

where $\mathbf{n}^{\text{el}}(x) = \psi_{\text{b}}(x)\psi_{\text{b}}^{\dagger}(x)$ is the local electronic bound-state density matrix and $n^{\text{el}}(x) = \text{tr}[\mathbf{n}^{\text{el}}(x)]$ is its associated density. The direct-Breit-type (DB) and exchange-Breit-type (XB) contributions are

$$\mathcal{E}_{\text{b}}^{\text{vp},(1),\text{DB}} = -\frac{1}{c^2} \int_{-\infty}^{\infty} j^{\text{el}}(x)j_{\text{ren}}^{\text{vp}}(x)dx, \quad (54)$$

and

$$\mathcal{E}_{\text{b}}^{\text{vp},(1),\text{XB}} = \frac{1}{c^2} \int_{-\infty}^{\infty} \text{tr}[\mathbf{j}^{\text{el}}(x)\mathbf{j}_{\text{ren}}^{\text{vp}}(x)]dx, \quad (55)$$

where $\mathbf{j}^{\text{el}}(x) = c\boldsymbol{\sigma}_1\mathbf{n}^{\text{el}}(x)$ and $\mathbf{j}_{\text{ren}}^{\text{vp}}(x) = c\boldsymbol{\sigma}_1\mathbf{n}_{\text{ren}}^{\text{vp}}(x)$ are the local electronic bound-state and renormalized vacuum-polarization current density matrices, and $j^{\text{el}}(x) = \text{tr}[\mathbf{j}^{\text{el}}(x)]$ and $j_{\text{ren}}^{\text{vp}}(x) = \text{tr}[\mathbf{j}_{\text{ren}}^{\text{vp}}(x)]$ are their associated current densities. By time-reversal symmetry, the current densities vanish, i.e. $j^{\text{el}}(x) = j_{\text{ren}}^{\text{vp}}(x) = 0$ (see, e.g., Ref. 76), and thus the DB contribution is zero, i.e. $\mathcal{E}_{\text{b}}^{\text{vp},(1),\text{DB}} = 0$.

Fig. 2 reports these QED corrections to the bound-state energy as a function of the inverse speed of light $1/c$, using the renormalized local vacuum-polarization density matrix [Eq. (49)] without and with the Dirac-delta contribution $-(\mathcal{N}_{\text{reg}}^{\text{vp}}/2)\delta(x)\mathbf{I}_2$. The total first-order QED correction is negative without the Dirac-delta contribution, but it becomes positive after adding it. Thus, the total effect of the vacuum polarization in the present model is to destabilize the bound-state energy. We note that, for the 3D hydrogen-like atom, the total QED energy correction on the ground-state energy is also positive, i.e. the ground state is also destabilized (see, e.g., Ref. 77). As regards now the different contributions to the total QED energy correction in the present model, we observe the a priori unexpected fact that the XC contribution vanishes and the DC and XB contributions are equal, when using the renormalized local vacuum-polarization density matrix.

III. FINITE-DIMENSIONAL APPROXIMATION TO THE 1D HYDROGEN-LIKE DIRAC MODEL

In this section, we study the 1D hydrogen-like Dirac model using a finite plane-wave basis.

A. Calculations in a finite plane-wave basis

We consider a finite-dimensional approximation of the Hilbert space with an infrared (IR) cutoff parameter L and an ultraviolet (UV) cutoff parameter Λ ,

$$\mathcal{H}^{L,\Lambda} = \text{span} \left(\{ \chi_n^L \}_{|n| \leq n_{\text{max}}} \cup \{ \chi_n^S \}_{|n| \leq n_{\text{max}}} \right), \quad (56)$$

which is spanned by a basis of large- and small-component plane-wave functions $\chi_n^L, \chi_n^S : [-L/2, L/2] \rightarrow \mathbb{C}^2$

$$\chi_n^L(x) = \frac{1}{\sqrt{L}} \begin{pmatrix} e^{ik_n x} \\ 0 \end{pmatrix} \quad \text{and} \quad \chi_n^S(x) = \frac{1}{\sqrt{L}} \begin{pmatrix} 0 \\ e^{ik_n x} \end{pmatrix}, \quad (57)$$

with $k_n = 2\pi n/L$ and $n_{\max} = \lfloor L\Lambda/(2\pi) \rfloor$. Physically, it corresponds to an electron on the interval $[-L/2, L/2]$ with maximal momentum $|k_{n_{\max}}| \leq \Lambda$. Ultimately, we will be interested in the limits $L \rightarrow \infty$ and $\Lambda \rightarrow \infty$.

Using Eq. (9), the 1D hydrogen-like Dirac eigenvalue equation, $\mathbf{D}_Z \psi_p^Z = \varepsilon_p^Z \psi_p^Z$, on this finite-dimensional Hilbert space leads to the following matrix eigenvalue equation

$$\begin{pmatrix} mc^2 \mathbf{I} + \mathbf{V} & c\mathbf{P} \\ c\mathbf{P} & -mc^2 \mathbf{I} + \mathbf{V} \end{pmatrix} \begin{pmatrix} \mathbf{c}_p^L \\ \mathbf{c}_p^S \end{pmatrix} = \varepsilon_p^Z \begin{pmatrix} \mathbf{c}_p^L \\ \mathbf{c}_p^S \end{pmatrix}, \quad (58)$$

where \mathbf{c}_p^L and \mathbf{c}_p^S are $(2n_{\max} + 1)$ -component vectors, and \mathbf{I} , \mathbf{P} , and \mathbf{V} are $(2n_{\max} + 1) \times (2n_{\max} + 1)$ matrices with elements

$$\mathbf{I}_{n,m} = \langle \chi_n^L, \chi_m^L \rangle_L = \langle \chi_n^S, \chi_m^S \rangle_L = \delta_{n,m}, \quad (59)$$

$$\mathbf{P}_{n,m} = \langle \chi_n^L, \sigma_{1p_x} \chi_m^S \rangle_L = \langle \chi_n^S, \sigma_{1p_x} \chi_m^L \rangle_L = k_n \delta_{n,m}, \quad (60)$$

and

$$\mathbf{V}_{n,m} = -Z \chi_n^{L\dagger}(0) \chi_m^L(0) = -Z \chi_n^{S\dagger}(0) \chi_m^S(0) = -\frac{Z}{L}, \quad (61)$$

where $\langle \cdot, \cdot \rangle_L$ denotes here the standard inner product in $L^2([-L/2, L/2], \mathbb{C}^2)$. Note that, since $\sigma_{1p_x} \chi_n^L = k_n \chi_n^S$ and $\sigma_{1p_x} \chi_n^S = k_n \chi_n^L$, the plane-wave basis satisfies the kinetic-balance condition in all its variants (see, e.g., Refs. 76, 78–83). This ensures that, as $c \rightarrow \infty$, the non-relativistic limit with the same basis is correctly reached. Moreover, by analogy with the 3D case, since the plane-wave basis is adapted to the free Dirac operator \mathbf{D}_0 , it is expected to avoid any spectral pollution [84, 85].

After solving Eq. (58), we obtain $4n_{\max} + 2$ eigenfunctions of the form

$$\psi_p^Z(x) = \sum_{n=-n_{\max}}^{n_{\max}} c_{p,n}^L \chi_n^L(x) + \sum_{n=-n_{\max}}^{n_{\max}} c_{p,n}^S \chi_n^S(x), \quad (62)$$

which can be partitioned into a set of positive-energy states (PS) $\{\psi_p^Z\}_{p \in \text{PS}}$ and a set of negative-energy states (NS) $\{\psi_p^Z\}_{p \in \text{NS}}$. The local vacuum-polarization density matrix can then be calculated as, for given IR cutoff parameter L and UV cutoff parameter Λ ,

$$\mathbf{n}_{L,\Lambda}^{\text{VP}}(x) = \sum_{p \in \text{NS}} \psi_p^Z(x) \psi_p^{Z\dagger}(x) - \sum_{p \in \text{PS}} \psi_p^0(x) \psi_p^{0\dagger}(x), \quad (63)$$

where $\{\psi_p^0\}$ are the eigenfunctions for $Z = 0$ calculated in the same basis. The corresponding vacuum-polarization density is $n_{L,\Lambda}^{\text{VP}}(x) = \text{tr}[\mathbf{n}_{L,\Lambda}^{\text{VP}}(x)]$.

B. Convergence of the bound-state energy and eigenfunction

Figure 3 reports the convergence of the bound-state energy as a function of the IR cutoff parameter L and the UV cutoff parameter Λ . As $L \rightarrow \infty$ and $\Lambda \rightarrow \infty$, the bound-state energy calculated in the plane-wave basis correctly converges to the exact value in Eq. (7). This supports the fact that the basis calculations based on Eq. (9) corresponds to the self-adjoint realization of the Hamiltonian \mathbf{D}_Z that we have selected via Eqs. (4)-(6). Numerically, we find that the bound-state energy converges exponentially as $L \rightarrow \infty$, and roughly as $1/\Lambda$ as $\Lambda \rightarrow \infty$. This is expected based on the theoretical analysis in Appendix D.

Figure 4 reports the convergence of the large and small components of the bound-state eigenfunction as a function of the IR cutoff parameter L and the UV cutoff parameter Λ . The large component of the exact eigenfunction [see Eq. (8)] has a derivative discontinuity at $x = 0$, and consequently the convergence with Λ is slow near $x = 0$. The small component of the exact eigenfunction [see Eq. (8)] has a discontinuity at $x = 0$, in addition of having the same

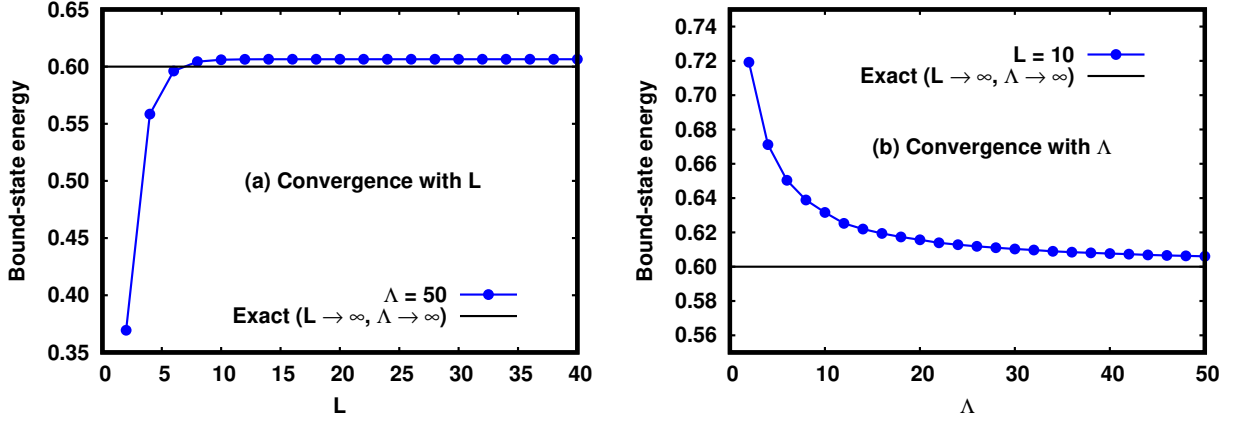


FIG. 3. Convergence of the bound-state energy of the 1D hydrogen-like Dirac model with a plane-wave basis as a function of (a) the IR cutoff parameter L and (b) the UV cutoff parameter Λ for $m = c = Z = 1$. The exact value in the limits $L \rightarrow \infty$ and $\Lambda \rightarrow \infty$ is $\varepsilon_b = 0.6$.

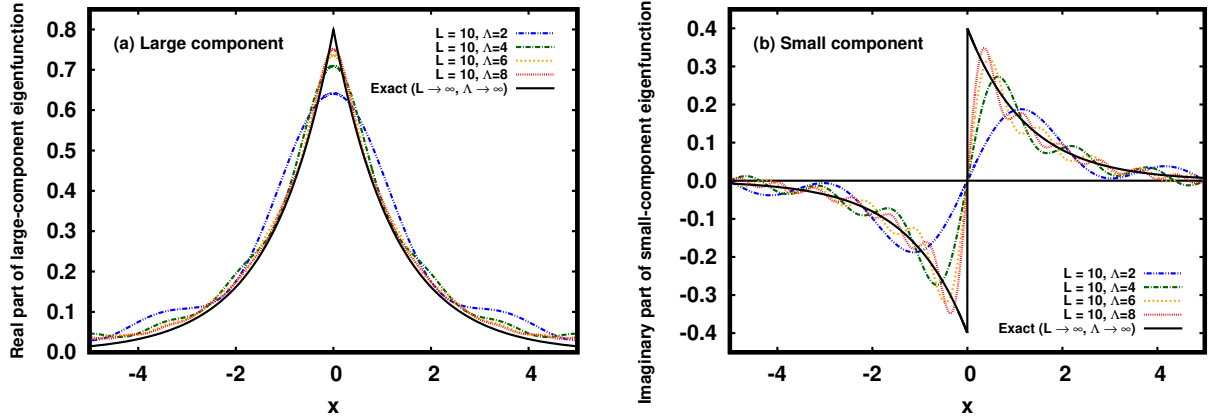


FIG. 4. Convergence of the (a) large component and (b) small component of the bound-state eigenfunction of the 1D hydrogen-like Dirac model with a plane-wave basis as a function of the UV cutoff parameter Λ for an IR cutoff parameter $L = 10$ and $m = c = Z = 1$. The exact eigenfunction [Eq. (8)] corresponds to the limits $L \rightarrow \infty$ and $\Lambda \rightarrow \infty$.

derivative discontinuity at $x = 0$ as the large component, and consequently the convergence with respect to Λ near $x = 0$ is even slower than for the large component. Note that this discontinuity at $x = 0$ of the exact small-component eigenfunction cannot be reproduced in the finite plane-wave basis, since the expansion of an odd function in a basis of continuous functions necessarily gives zero at $x = 0$. This implies that the finite plane-wave basis always incorrectly gives a vanishing small-component contribution to the bound-state density at $x = 0$. As seen from the analysis in Appendix D, the convergence of the small-component eigenfunction is the limiting factor in the convergence of the bound-state energy as $\Lambda \rightarrow \infty$. Naively, this last fact might lead one to think that a faster convergence of the bound-state energy with respect to Λ would be obtained in the non-relativistic limit since only the large component survives in this limit. In fact, it can be shown that, in the non-relativistic limit, the bound-state energy still converges as $1/\Lambda$ as $\Lambda \rightarrow \infty$. This is because the non-relativistic Hamiltonian involves now the second-order derivative of the large-component eigenfunction (see, also, Ref. 44 for a related discussion on the basis convergence of the non-relativistic bound-state energy).

C. Convergence of the vacuum-polarization density

We now discuss the convergence of the total vacuum-polarization density $n_{L,\Lambda}^{\text{VP}}(x)$ calculated from Eq. (63) with a finite plane-wave basis. Since in our finite plane-wave basis, we obtain the same number of negative-energy states for a non-vanishing nuclear charge $Z < 2c$ and $Z = 0$, the basis-set total vacuum-polarization density necessarily

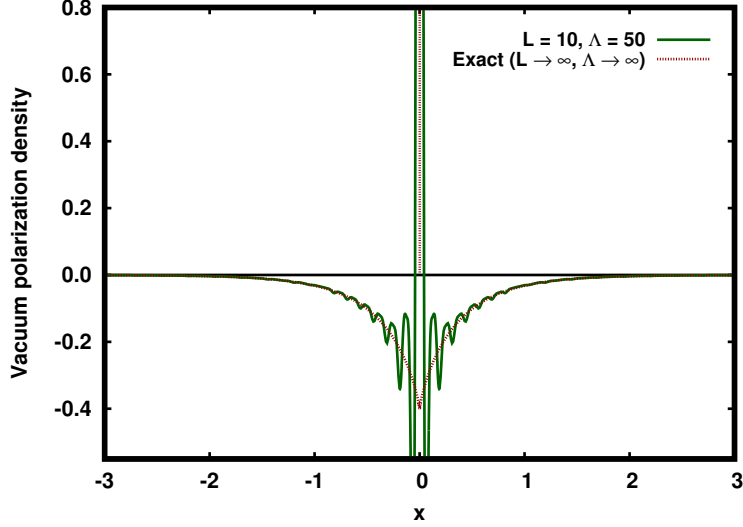


FIG. 5. The total vacuum-polarization density for $m = c = Z = 1$, calculated exactly [Eq. (48)] and with a plane-wave basis for a IR cutoff parameter $L = 10$ and a UV cutoff parameter $\Lambda = 50$ [from Eq. (63)].

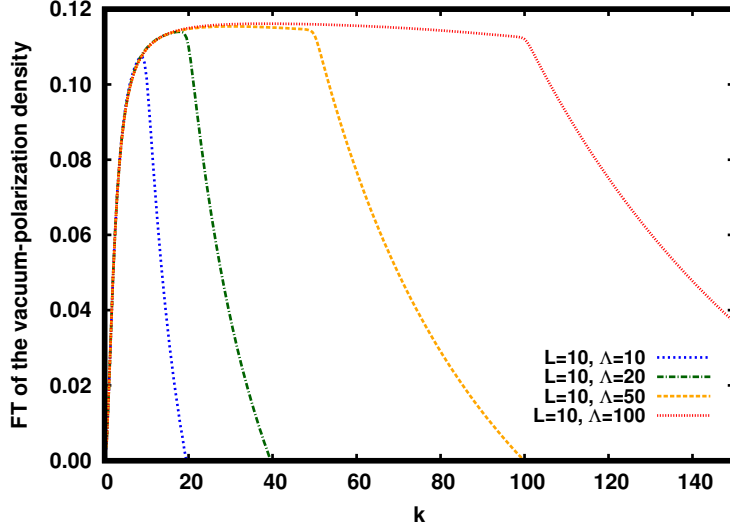


FIG. 6. Fourier transform of the total vacuum-polarization density calculated with a plane-wave basis [Eq. (64)] for a IR cutoff parameter $L = 10$ and different UV cutoff parameters Λ for $m = c = Z = 1$.

integrates to zero for any finite cutoff parameters L and Λ , i.e. $\int_{-\infty}^{\infty} n_{L,\Lambda}^{\text{VP}}(x)dx = 0$. Thus, we can consider that the basis-set calculation does not give an approximation to the total vacuum-polarization density in Eq. (42), which does not integrate to zero, but rather it gives directly an approximation to the renormalized total vacuum-polarization density in Eq. (48), which does integrate to zero.

The total vacuum-polarization density $n_{L,\Lambda}^{\text{VP}}(x)$ calculated with a plane-wave basis with a IR cutoff parameter $L = 10$ and a UV cutoff parameter $\Lambda = 50$ is reported in Fig. 5, and compared with the exact one [Eq. (48)]. The plane-wave basis calculation reproduces well the vacuum-polarization density for large enough x . However, the plane-wave basis generates large oscillations near $x = 0$ while trying to reproduce the Dirac-delta contribution in Eq. (48), resulting in an effectively impossible pointwise convergence of the vacuum-polarization density near $x = 0$.

To analyze this convergence problem, we report in Fig. 6 the Fourier transform of the total vacuum-polarization density calculated with the plane-wave basis

$$\hat{n}_{L,\Lambda}^{\text{VP}}(k) = \frac{1}{\sqrt{2\pi}} \int_{-L/2}^{L/2} n_{L,\Lambda}^{\text{VP}}(x) e^{-ikx} dx. \quad (64)$$

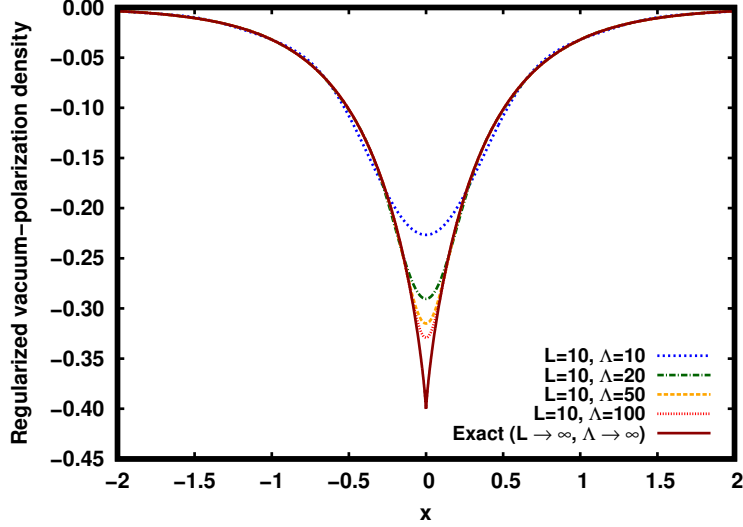


FIG. 7. Regularized total vacuum-polarization density [Eq. (67)] for $m = c = Z = 1$ calculated in a plane-wave basis for a IR cutoff parameter $L = 10$ and different UV cutoff parameters Λ , compared to the exact regular part of the total vacuum-polarization density.

To reproduce the Dirac-delta contribution to the vacuum-polarization density in position space, $\hat{n}_{L,\Lambda}^{\text{VP}}(k)$ should tend to a constant as $k \rightarrow \infty$. However, with a finite UV cutoff parameter Λ , the Fourier transform $\hat{n}_{L,\Lambda}^{\text{VP}}(k)$ is only able to approximately converge to a constant for $k \lesssim \Lambda$, but for $k \gtrsim \Lambda$ quickly decays to reach zero at $k = 2\Lambda$. Note that the reason why $\hat{n}_{L,\Lambda}^{\text{VP}}(k)$ is not zero for $\Lambda \leq k \leq 2\Lambda$ is that, according to Eq. (63), $\hat{n}_{L,\Lambda}^{\text{VP}}(k)$ involves the product of two plane waves, each with momenta going up to Λ . However, $\hat{n}_{L,\Lambda}^{\text{VP}}(k)$ cannot be expected to be accurate for the momentum range $\Lambda < k \leq 2\Lambda$ since contributions from plane waves with momenta greater than Λ are missing.

This suggests the following simple scheme to extract the regular part of the vacuum-polarization density in a finite basis. For given L and Λ , we select a maximal momentum k_{max} , and truncate $\hat{n}_{L,\Lambda}^{\text{VP}}(k) - \hat{n}_{L,\Lambda}^{\text{VP}}(k_{\text{max}})$ for $|k| > k_{\text{max}}$, i.e.

$$\hat{n}_{\text{reg},L,\Lambda}^{\text{VP}}(k) = \left[\hat{n}_{L,\Lambda}^{\text{VP}}(k) - \hat{n}_{L,\Lambda}^{\text{VP}}(k_{\text{max}}) \right] \theta(k_{\text{max}} - |k|). \quad (65)$$

By construction, $\hat{n}_{\text{reg},L,\Lambda}^{\text{VP}}(k)$ is thus zero for $|k| > k_{\text{max}}$. In practice, we choose for k_{max} the value of k at which $\hat{n}_{L,\Lambda}^{\text{VP}}(k)$ reaches its maximum, i.e.

$$k_{\text{max}} = \underset{k \in [0, 2\Lambda]}{\text{argmax}} \hat{n}_{L,\Lambda}^{\text{VP}}(k). \quad (66)$$

The values of k_{max} obtained in this way are close to Λ . The choice of k_{max} in Eq. (66), instead of the simpler choice $k_{\text{max}} = \Lambda$, has the advantage that it leads to $\hat{n}_{\text{reg},L,\Lambda}^{\text{VP}}$ having a continuous vanishing derivative at $k = k_{\text{max}}$. We finally take the inverse Fourier transform of $\hat{n}_{\text{reg},L,\Lambda}^{\text{VP}}(k)$, i.e.

$$n_{\text{reg},L,\Lambda}^{\text{VP}}(x) = \frac{1}{\sqrt{2\pi}} \int_{-k_{\text{max}}}^{k_{\text{max}}} \hat{n}_{\text{reg},L,\Lambda}^{\text{VP}}(k) e^{ikx} dk, \quad (67)$$

resulting in a regularized vacuum-polarization density where the approximation of the Dirac-delta contribution in the finite basis has been removed. This quantity should then converge to the regular part of the total vacuum-polarization density as $L \rightarrow \infty$ and $\Lambda \rightarrow \infty$, i.e. $\lim_{L \rightarrow \infty} \lim_{\Lambda \rightarrow \infty} n_{\text{reg},L,\Lambda}^{\text{VP}}(x) = n_{\text{reg}}^{\text{VP}}(x)$. Moreover, from the value $\hat{n}_{L,\Lambda}^{\text{VP}}(k_{\text{max}})$, we get directly the integral of $n_{\text{reg},L,\Lambda}^{\text{VP}}(x)$

$$\begin{aligned} \mathcal{N}_{\text{reg},L,\Lambda}^{\text{VP}} &= \int_{-L/2}^{L/2} n_{\text{reg},L,\Lambda}^{\text{VP}}(x) dx \\ &= \sqrt{2\pi} \hat{n}_{\text{reg},L,\Lambda}^{\text{VP}}(0) \\ &= -\sqrt{2\pi} \hat{n}_{L,\Lambda}^{\text{VP}}(k_{\text{max}}). \end{aligned} \quad (68)$$

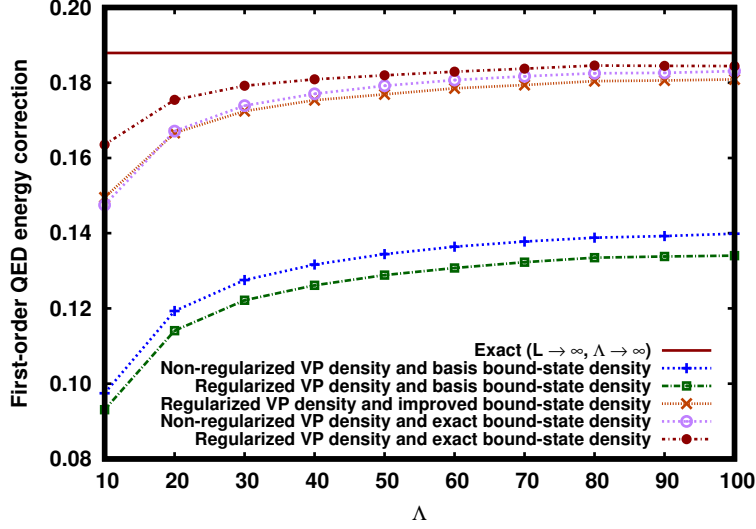


FIG. 8. Convergence of the first-order QED correction to the bound-state energy calculated in a plane-wave basis as a function of the UV cutoff parameter Λ for a IR cutoff parameter $L = 10$ and for $m = c = Z = 1$, using either the non-regularized vacuum-polarization density matrix $\mathbf{n}_{L,\Lambda}^{\text{VP}}(x)$ [Eq. (63)] or the regularized renormalized vacuum-polarization density matrix $\mathbf{n}_{\text{ren},L,\Lambda}^{\text{VP}}(x)$ [Eq. (70)], and the finite-basis bound-state density matrix $\mathbf{n}_{L,\Lambda}^{\text{el}}(x)$ or a version of it with an improved density at $x = 0$ (see Section III D) or the exact bound-state density matrix $\mathbf{n}^{\text{el}}(x)$.

The renormalized total vacuum-polarization density in Eq. (48) can thus be approximated from the finite basis calculation as

$$n_{\text{ren},L,\Lambda}^{\text{VP}}(x) = -\mathcal{N}_{\text{reg},L,\Lambda}^{\text{VP}} \delta(x) + n_{\text{reg},L,\Lambda}^{\text{VP}}(x). \quad (69)$$

The regularized vacuum-polarization density $n_{\text{reg},L,\Lambda}^{\text{VP}}(x)$ obtained by the above scheme is reported in Fig. 7 for different UV cutoff parameters Λ . We see that our regularization scheme has properly eliminated the large oscillations near $x = 0$ and the regularized vacuum-polarization density converges indeed toward the regular part of the exact vacuum-polarization density as the UV cutoff is increased. However, this convergence remains slow near $x = 0$ due to the fact that the regular part of the exact vacuum-polarization density has an infinite derivative discontinuity at $x = 0$.

D. Convergence of the QED correction to the bound-state energy

In Fig. 8, we report the convergence of the total first-order QED correction to the bound-state energy in Eq. (51) calculated in different ways in the plane-wave basis as a function of the UV cutoff parameter Λ . The first and most straightforward way of calculating this QED correction is to use in Eqs. (52)-(55) the non-regularized vacuum-polarization density matrix $\mathbf{n}_{L,\Lambda}^{\text{VP}}(x)$ in Eq. (63) for given cutoff parameters L and Λ , together with the bound-state electronic density matrix $\mathbf{n}_{L,\Lambda}^{\text{el}}(x)$ calculated with the same cutoff parameters. The QED correction calculated in this way converges so slowly with respect to Λ that it is not even possible to check numerically that it eventually goes to the exact value as $\Lambda \rightarrow \infty$. The second way of calculating the QED correction is to approximate the renormalized local vacuum-polarization density matrix in Eq. (49) by

$$\mathbf{n}_{\text{ren},L,\Lambda}^{\text{VP}}(x) = -\frac{\mathcal{N}_{\text{reg},L,\Lambda}^{\text{VP}}}{2} \delta(x) \mathbf{I}_2 + \mathbf{n}_{\text{reg},L,\Lambda}^{\text{VP}}(x), \quad (70)$$

where $\mathbf{n}_{\text{reg},L,\Lambda}^{\text{VP}}(x)$ is a regularized local vacuum-polarization density matrix that we define in momentum space as, similarly to Eq. (65),

$$\hat{\mathbf{n}}_{\text{reg},L,\Lambda}^{\text{VP}}(k) = \left[\hat{\mathbf{n}}_{L,\Lambda}^{\text{VP}}(k) - \hat{\mathbf{n}}_{L,\Lambda}^{\text{VP}}(k_{\text{max}}) \right] \theta(k_{\text{max}} - |k|), \quad (71)$$

using the same value for k_{max} as the one used for the vacuum-polarization density [see Eq. (66)]. It turns out that the QED correction calculated in this way does not converge any faster and is in fact for finite Λ slightly further away

from the exact value than the QED correction calculated with the non-regularized local vacuum-polarization density matrix.

The large errors on the QED correction to the bound-state energy observed for finite Λ both when using the non-regularized and regularized local vacuum-polarization density matrices actually come from a too poor description of the bound-state density matrix in the finite plane-wave basis, and in particular an incorrect value of the bound-state density at $x = 0$. Indeed, as mentioned in Section III B, the finite plane-wave basis gives an incorrect vanishing small-component contribution to the bound-state density, which largely affects the QED correction to the bound-state energy. A better estimate of the small-component bound-state density at $x = 0$ is given by maximal value of the small-component bound-state density, which is reached near $x = 0$ but not at $x = 0$. We can then use this improved estimate for the bound-state density at $x = 0$ for calculating the delta contribution to the QED correction when using the regularized local vacuum-polarization density matrix in Eq. (70). The resulting QED correction calculated in this way, reported in Fig. 8, has much smaller errors for any finite Λ . Note, however, that this improved value of the bound-state density at $x = 0$ cannot be used with the non-regularized local vacuum-polarization density matrix which does not have a delta contribution. Finally, in Fig. 8, we also show the QED correction to the bound-state energy calculated with the exact bound-state density matrix $\mathbf{n}^{\text{el}}(x)$ and with either the non-regularized or the regularized local vacuum-polarization density matrix. The obtained curves are quite similar to the one obtained with the improved bound-state density at $x = 0$.

IV. CONCLUSION

In this work, we have reexamined the 1D effective QED model of the hydrogen-like atom with delta-potential interactions. We have provided some mathematical details on the definition of this model. We have calculated the exact vacuum-polarization density and density matrix, using momentum-space Green-function techniques, showing that a Dirac-delta contribution was missed in previous calculations. We have calculated the resulting Lamb-type shift of the bound-state energy. We have also studied the approximation of this model in a finite plane-wave basis, in particular the basis convergence of the bound-state energy and eigenfunction, of the vacuum-polarization density, of the Lamb-type shift of the bound-state energy. We have shown that it is difficult to converge the vacuum-polarization density with respect to the UV momentum cutoff of the plane-wave basis due to the presence of the Dirac-delta contribution. We have proposed a way of filtering out in momentum space this Dirac-delta contribution in the plane-wave calculations in order to converge the regular part of the vacuum-polarization density in the basis.

We believe that the present work may give some hints on how to perform finite-basis calculations of the vacuum-polarization density of atoms and molecules in the 3D effective QED theory with Coulomb interactions. Indeed, for atoms and molecules, the calculation of the vacuum-polarization density in a finite basis presents similar problems as in the present 1D model. For instance, the vacuum-polarization density of an atom with a point-charge nucleus also contains a Dirac-delta contribution at the nucleus (see, e.g., Refs. 40 and 62). A similar regularization technique in momentum space as the one used in the present work may be therefore useful in this case as well. We hope to confirm this in a future work.

Appendix A: Matrix elements of the 1D hydrogen-like Dirac Hamiltonian

In this appendix, we argue that the matrix elements of the 1D hydrogen-like Dirac Hamiltonian \mathbf{D}_Z can be defined on a set of functions larger than its domain.

We start from the definition of the Hamiltonian \mathbf{D}_Z as having the same action of the free Dirac Hamiltonian \mathbf{D}_0 for $x \neq 0$, i.e.

$$\mathbf{D}_Z \psi = \mathbf{D}_0 \psi \quad \text{on } \mathbb{R} \setminus \{0\}. \quad (\text{A1})$$

with the Z -dependent domain

$$\text{Dom}(\mathbf{D}_Z) = \{ \psi \in H^1(\mathbb{R} \setminus \{0\}, \mathbb{C}^2) \mid \psi(0^+) = \mathbf{M}_Z \psi(0^-) \}, \quad (\text{A2})$$

where the matrix \mathbf{M}_Z is defined in Eq. (6). Let us consider two functions ψ and ϕ in $\text{Dom}(\mathbf{D}_Z)$. Since they have a discontinuity at $x = 0$, they can be written as, for $x \in \mathbb{R}$,

$$\psi(x) = \psi_-(x) + H(x) [\psi_+(x) - \psi_-(x)] \quad \text{and} \quad \phi(x) = \phi_-(x) + H(x) [\phi_+(x) - \phi_-(x)], \quad (\text{A3})$$

where H is the Heaviside-step function, and ψ_{\pm} and ϕ_{\pm} are (non-unique) functions in $H^1(\mathbb{R}, \mathbb{C}^2)$ such that $\psi_- = \psi$ and $\phi_- = \phi$ on \mathbb{R}^- and $\psi_+ = \psi$ and $\phi_+ = \phi$ on \mathbb{R}^+ . Since they are chosen in $H^1(\mathbb{R}, \mathbb{C}^2)$, the functions ψ_{\pm} and ϕ_{\pm} are continuous at $x = 0$ and we have $\psi_{\pm}(0) = \psi(0^{\pm})$ and $\phi_{\pm}(0) = \phi(0^{\pm})$. The matrix element $\langle \phi, \mathbf{D}_Z \psi \rangle$ can be written as

$$\langle \phi, \mathbf{D}_Z \psi \rangle = \int_{-\infty}^0 \phi_-^\dagger(x) \mathbf{D}_0 \psi_-(x) dx + \int_0^{\infty} \phi_+^\dagger(x) \mathbf{D}_0 \psi_+(x) dx. \quad (\text{A4})$$

We would like to rewrite Eq. (A4) as a single integral over $(-\infty, +\infty)$ of $\phi^\dagger(x) \mathbf{D}_0 \psi(x)$ but the problem is that $\phi^\dagger(x) \mathbf{D}_0 \psi(x)$ formally contains a multiplication of distributions, namely the product of a Heaviside-step distribution and a Dirac-delta distribution, which is meaningless in the standard theory of distributions (where only the product of a distribution by a smooth function is defined). One way around this, in the spirit of Colombeau's generalized functions [47, 86–88], is to introduce regularized functions ψ_ϵ and ϕ_ϵ depending on a regularization parameter $\epsilon > 0$

$$\psi_\epsilon(x) = \psi_-(x) + H_\epsilon(x) [\psi_+(x) - \psi_-(x)] \quad \text{and} \quad \phi_\epsilon(x) = \phi_-(x) + H_\epsilon(x) [\phi_+(x) - \phi_-(x)], \quad (\text{A5})$$

where $H_\epsilon(x)$ is a regularized Heaviside-step function obtained by convoluting H with $\eta_\epsilon : x \mapsto (1/\epsilon)\eta(x/\epsilon)$

$$H_\epsilon(x) = (H * \eta_\epsilon)(x) = \int_{-\infty}^{+\infty} H(x-y) \frac{1}{\epsilon} \eta\left(\frac{y}{\epsilon}\right) dy, \quad (\text{A6})$$

where η is a mollifier, i.e. a compactly supported smooth real function satisfying $\int_{-\infty}^{\infty} \eta(x) dx = 1$. The derivative of ψ_ϵ is then

$$\psi'_\epsilon(x) = \psi'_-(x) + H_\epsilon(x) [\psi'_+(x) - \psi'_-(x)] + \delta_\epsilon(x) [\psi_+(x) - \psi_-(x)], \quad (\text{A7})$$

where $\delta_\epsilon = H'_\epsilon$ is the corresponding regularized Dirac-delta function

$$\delta_\epsilon(x) = (\delta * \eta_\epsilon)(x) = \frac{1}{\epsilon} \eta\left(\frac{x}{\epsilon}\right). \quad (\text{A8})$$

Obviously, the limit $\epsilon \rightarrow 0$ corresponds to the non-regularized case with $\lim_{\epsilon \rightarrow 0} H_\epsilon = H$ and $\lim_{\epsilon \rightarrow 0} \delta_\epsilon = \delta$ in the sense of distributions. Now, since the regularized functions ψ_ϵ and ϕ_ϵ are in $H^1(\mathbb{R}, \mathbb{C}^2)$, we can integrate $\phi_\epsilon^\dagger(x) \mathbf{D}_0 \psi_\epsilon(x)$ over $(-\infty, +\infty)$ and take the limit $\epsilon \rightarrow 0$

$$\lim_{\epsilon \rightarrow 0} \int_{-\infty}^{\infty} \phi_\epsilon^\dagger(x) \mathbf{D}_0 \psi_\epsilon(x) dx = \langle \phi, \mathbf{D}_Z \psi \rangle + S, \quad (\text{A9})$$

where the regular part (not involving a delta function) of the integrand gives the value $\langle \phi, \mathbf{D}_Z \psi \rangle$ in Eq. (A4) and the singular part (involving a delta function) of the integrand gives an additional contribution

$$S = \lim_{\epsilon \rightarrow 0} \int_{-\infty}^{\infty} -ic \left[\phi_-^\dagger(x) + H_\epsilon(x) [\phi_+^\dagger(x) - \phi_-^\dagger(x)] \right] \sigma_1 \delta_\epsilon(x) [\psi_+(x) - \psi_-(x)] dx. \quad (\text{A10})$$

The difficult term in this expression is the one involving the product $H_\epsilon(x)\delta_\epsilon(x)$ that we calculate now for any continuous and integrable function $f : \mathbb{R} \rightarrow \mathbb{C}$

$$\begin{aligned} \lim_{\epsilon \rightarrow 0} \int_{-\infty}^{\infty} H_\epsilon(x)\delta_\epsilon(x)f(x)dx &= \lim_{\epsilon \rightarrow 0} \int_{-\infty}^{\infty} \int_{-\infty}^{\infty} H(x-y)\frac{1}{\epsilon}\eta\left(\frac{y}{\epsilon}\right)\frac{1}{\epsilon}\eta\left(\frac{x}{\epsilon}\right)f(x)dx dy \\ &= \lim_{\epsilon \rightarrow 0} \int_{-\infty}^{\infty} \int_{-\infty}^{\infty} H(x-y)\eta(y)\eta(x)f(\epsilon x)dx dy \\ &= af(0), \end{aligned} \tag{A11}$$

where the real number a is given by

$$\begin{aligned} a &= \int_{-\infty}^{\infty} \int_{-\infty}^{\infty} H(x-y)\eta(x)\eta(y)dx dy = \int_{-\infty}^{\infty} \int_{-\infty}^{\infty} [1-H(y-x)]\eta(x)\eta(y)dx dy \\ &= 1 - \int_{-\infty}^{\infty} \int_{-\infty}^{\infty} H(y-x)\eta(x)\eta(y)dx dy \\ &= 1 - a, \end{aligned} \tag{A12}$$

i.e., $a = 1/2$ independently of the mollifier η . Thus, we have shown that $\lim_{\epsilon \rightarrow 0} H_\epsilon\delta_\epsilon = (1/2)\delta$ in the sense of distributions, which corresponds to the result obtained in Colombeau theory. Notice that the value $a = 1/2$ is obtained only if we use the same regularized Heaviside-step function H_ϵ for both ψ_ϵ and ϕ_ϵ in Eq. (A5). Using Eq. (A11), the term S in Eq. (A10) simplifies to

$$\begin{aligned} S &= -\frac{ic}{2} [\phi_+^\dagger(0) + \phi_-^\dagger(0)] \sigma_1 [\psi_+(0) - \psi_-(0)] \\ &= -\frac{ic}{2} [\phi^\dagger(0^+) + \phi^\dagger(0^-)] \sigma_1 [\psi(0^+) - \psi(0^-)]. \end{aligned} \tag{A13}$$

Using now the boundary condition $\psi(0^+) = \mathbf{M}_Z\psi(0^-)$ and the matrix identity $-ic\sigma_1[\mathbf{M}_Z - \mathbf{I}_2] = (Z/2)[\mathbf{M}_Z + \mathbf{I}_2]$, we can write S as

$$\begin{aligned} S &= -\frac{ic}{2} [\phi^\dagger(0^+) + \phi^\dagger(0^-)] \sigma_1 [\mathbf{M}_Z - \mathbf{I}_2] \psi(0^-) \\ &= \frac{Z}{4} [\phi^\dagger(0^+) + \phi^\dagger(0^-)] [\mathbf{M}_Z + \mathbf{I}_2] \psi(0^-) \\ &= \frac{Z}{4} [\phi^\dagger(0^+) + \phi^\dagger(0^-)] [\psi(0^+) + \psi(0^-)] \\ &= Z\bar{\phi}^\dagger(0)\bar{\psi}(0), \end{aligned} \tag{A14}$$

where we have defined $\bar{\psi}(0) = [\psi(0^+) + \psi(0^-)]/2$ and $\bar{\phi}(0) = [\phi(0^+) + \phi(0^-)]/2$. Therefore, we arrive at the following expression for $\langle \phi, \mathbf{D}_Z\psi \rangle$

$$\langle \phi, \mathbf{D}_Z\psi \rangle = \lim_{\epsilon \rightarrow 0} \int_{-\infty}^{\infty} \phi_\epsilon^\dagger(x)\mathbf{D}_0\psi_\epsilon(x)dx - Z\bar{\phi}^\dagger(0)\bar{\psi}(0). \tag{A15}$$

If we define the matrix element $\langle \phi, \mathbf{D}_0\psi \rangle$ using the regularized functions, or equivalently in Fourier space,

$$\langle \phi, \mathbf{D}_0\psi \rangle = \lim_{\epsilon \rightarrow 0} \int_{-\infty}^{\infty} \phi_\epsilon^\dagger(x)\mathbf{D}_0\psi_\epsilon(x)dx = \int_{-\infty}^{\infty} \hat{\phi}^\dagger(k)[c\sigma_1 k + \sigma_3 mc^2]\hat{\psi}(k)dk, \tag{A16}$$

where $\hat{\psi}$ and $\hat{\phi}$ are the Fourier transforms of ψ and ϕ , respectively, we can finally write $\langle \phi, \mathbf{D}_Z\psi \rangle$ as

$$\langle \phi, \mathbf{D}_Z\psi \rangle = \langle \phi, \mathbf{D}_0\psi \rangle - Z\bar{\phi}^\dagger(0)\bar{\psi}(0). \tag{A17}$$

Thus, the potential term in Eq. (A17) corresponds to interpreting the multiplication of the delta function $\delta(x)$ with a function $\psi(x)$ discontinuous at $x = 0$ as $\delta(x)\psi(x) = \bar{\psi}(0)\delta(x)$, as done in Refs. 45–47. This can also be understood from a distribution theory for discontinuous test functions [89]. Using the bound-state eigenfunction ψ_b^Z in Eq. (8), it can be explicitly checked that calculating $\langle \psi_b^Z, \mathbf{D}_Z\psi_b^Z \rangle$ using Eq. (A17) correctly gives the bound-state energy ε_b^Z in Eq. (7). We argue that Eq. (A17) can be used to define the matrix elements of the Hamiltonian \mathbf{D}_Z on a Z -independent set of functions larger than its domain, and in particular containing continuous functions.

The formal Dirac Hamiltonian with a delta-function potential in Eq. (1) has also been interpreted in various works [48, 55, 90–92] as another self-adjoint operator D'_ζ corresponding to another boundary condition which has the same form as Eq. (6) but with θ replaced by $\theta' = \zeta/c$ for $0 \leq \zeta < c\pi$. In this case, Eq. (A17) becomes

$$\langle \phi, D'_\zeta \psi \rangle = \langle \phi, D_0 \psi \rangle - 2c \tan\left(\frac{\zeta}{2c}\right) \bar{\phi}^\dagger(0) \bar{\psi}(0). \quad (\text{A18})$$

This operator D'_ζ is thus identical to the operator $D_{Z(\zeta)}$ considered in the present work with the nuclear charge $Z(\zeta) = 2c \tan(\zeta/2c)$. The reason why the operator D'_ζ is sometimes considered to be a realization of Eq. (1) is that, if we take a family of local regular real-valued potentials $v_\epsilon(x) = v(x/\epsilon)/\epsilon$ with $\int_{-\infty}^{\infty} v(x) dx = 1$ that converges (in the distribution sense) to the Dirac-delta function $\delta(x)$ as $\epsilon \rightarrow 0$, then the family of Dirac operators $D_{\zeta, \epsilon}^{\text{local}}$ with these local potentials $-\zeta v_\epsilon$ converges (in the norm-resolvent sense) to D'_ζ as $\epsilon \rightarrow 0$ [50, 52, 53, 90, 91, 93–95]

$$D_{\zeta, \epsilon}^{\text{local}} = D_0 - \zeta v_\epsilon \xrightarrow{\epsilon \rightarrow 0} D'_\zeta = D_{Z(\zeta)}. \quad (\text{A19})$$

The fact that $D_{\zeta, \epsilon}^{\text{local}}$ does not converge to D_ζ but to $D_{Z(\zeta)}$ is surprising. Instead, if we consider a family of Dirac operators $D_{Z, \epsilon}^{\text{nonlocal}}$ with the nonlocal potentials $-Z|v_\epsilon\rangle\langle v_\epsilon|$, where $v_\epsilon(x)$ still converges to the Dirac-delta function $\delta(x)$ as $\epsilon \rightarrow 0$, then $D_{Z, \epsilon}^{\text{nonlocal}}$ converges (in the norm-resolvent sense), as expected, to D_Z as $\epsilon \rightarrow 0$ [50, 89, 90, 94, 96–98]

$$D_{Z, \epsilon}^{\text{nonlocal}} = D_0 - Z|v_\epsilon\rangle\langle v_\epsilon| \xrightarrow{\epsilon \rightarrow 0} D_Z. \quad (\text{A20})$$

In a finite basis $\{\chi_n\}$ of functions that are continuous at $x = 0$, the matrix elements of the local and nonlocal operators $D_{Z, \epsilon}^{\text{local}}$ and $D_{Z, \epsilon}^{\text{nonlocal}}$ both reduce, in the limit $\epsilon \rightarrow 0$, to the matrix elements of the operator D_Z as given in Eq. (A17), i.e.

$$\lim_{\epsilon \rightarrow 0} \langle \chi_n, D_{Z, \epsilon}^{\text{local}} \chi_m \rangle = \lim_{\epsilon \rightarrow 0} \langle \chi_n, D_{Z, \epsilon}^{\text{nonlocal}} \chi_m \rangle = \langle \chi_n, D_0 \chi_m \rangle - Z \chi_n^\dagger(0) \chi_m(0) = \langle \chi_n, D_Z \chi_m \rangle. \quad (\text{A21})$$

Appendix B: Green function from an asymmetric UV momentum cutoff

In this appendix, we calculate the Green function that would have been obtained if we had used an asymmetric UV momentum cutoff in Section II B 1.

We consider a momentum interval $I(\Lambda) = [k_1(\Lambda), k_2(\Lambda)]$ containing 0 and such that $\lim_{\Lambda \rightarrow \infty} k_1(\Lambda) = -\infty$ and $\lim_{\Lambda \rightarrow \infty} k_2(\Lambda) = +\infty$, but which is not necessarily symmetric around 0, e.g. $I(\Lambda) = [-\Lambda, 2\Lambda]$. The calculation in Section II B 1 corresponds to using the symmetric interval $I(\Lambda) = [-\Lambda, \Lambda]$. Following the same steps as in the calculation in Section II B 1, we obtain for the variation of the Green function

$$\Delta G_Z(p, p'; \omega) = -\frac{Z}{2\pi} \bar{G}_0(p; \omega) \left[\mathbf{I}_2 + \frac{Z}{2\pi} \bar{G}_0(\omega) \right]^{-1} \bar{G}_0(p'; \omega), \quad (\text{B1})$$

where $\bar{G}_0(p; \omega)$ is given in Eq. (19) and $\bar{G}_0(\omega) = \int_{I(\Lambda)} \bar{G}_0(p; \omega) dp$. In the limit $\Lambda \rightarrow \infty$, we obtain

$$\lim_{\Lambda \rightarrow \infty} \bar{G}_0(\omega) = \frac{\pi}{c} \begin{pmatrix} -g(\omega) & a \\ a & g(-\omega) \end{pmatrix}, \quad (\text{B2})$$

with

$$a = \frac{c}{\pi} \lim_{\Lambda \rightarrow \infty} \int_{I(\Lambda)} \frac{cp}{\omega^2 - \varepsilon_p^2} dp. \quad (\text{B3})$$

Depending on the choice of $I(\Lambda)$, the constant a can be infinite or a finite real number independent of ω . To see this, we note that the off-diagonal elements of $\bar{G}_0(p; \omega)$ can be written as

$$\frac{cp}{\omega^2 - \varepsilon_p^2} = -\frac{1}{cp} H(|p| - 1) + R(p, \omega), \quad (\text{B4})$$

where H is the Heaviside-step function and R is an odd function in p and integrable in p over $(-\infty, +\infty)$. Thus, in the limit $\Lambda \rightarrow \infty$, the integral of $R(p, \omega)$ over p vanishes, and it remains

$$\begin{aligned} a &= -\frac{1}{\pi} \lim_{\Lambda \rightarrow \infty} \int_{I(\Lambda)} \frac{1}{p} H(|p| - 1) dp \\ &= -\frac{1}{\pi} \lim_{\Lambda \rightarrow \infty} \ln \left(\frac{k_2(\Lambda)}{-k_1(\Lambda)} \right). \end{aligned} \quad (\text{B5})$$

For example, for the asymmetric interval $I = [-\Lambda, 2\Lambda]$, we have $a = -(\ln 2)/\pi$. For a symmetric interval, i.e. $k_2(\Lambda) = -k_1(\Lambda)$, we recover $a = 0$.

Thus, we obtain, in the limit $\Lambda \rightarrow \infty$, a Green function with an arbitrary parameter $a \in \mathbb{R}$, whose value depends on how the infinite UV momentum limit is taken. In position space, we can extract from this Green function its associated boundary-condition matrix at $x = 0$

$$\mathbf{M}_Z^a = \frac{1}{1 - (a - i)^2 \lambda^2} \begin{pmatrix} 1 - (a^2 + 1)\lambda^2 & 2i\lambda \\ 2i\lambda & 1 - (a^2 + 1)\lambda^2 \end{pmatrix}, \quad (\text{B6})$$

with $\lambda = Z/2c$. This matrix can be rewritten in the form (see Ref. 51)

$$\mathbf{M}_Z^a = w \begin{pmatrix} A & iB \\ -iC & D \end{pmatrix}, \quad (\text{B7})$$

where $w = (1 - (a + i)^2 \lambda^2)/(1 - (a - i)^2 \lambda^2)$, $A = D = (1 - (a^2 + 1)\lambda^2)/\sqrt{P}$, $B = -C = 2\lambda/\sqrt{P}$, and $P = 1 - 2(a^2 - 1)\lambda^2 + (a^2 + 1)^2 \lambda^4$. It can be checked that $|w| = 1$, $AD - BC = 1$, and $A, B, C, D \in \mathbb{R}$. For $a \neq 0$, the obtained Green function corresponds to a self-adjoint Dirac Hamiltonian with a point-interaction potential [51], but different from the one defined by the boundary condition in Eq. (5). For $a = 0$, we recover the boundary condition in Eq. (5). This shows the importance of choosing a symmetric UV momentum cutoff to obtain the Green function corresponding to the Hamiltonian in Section II A.

Appendix C: Error in the calculation of the vacuum-polarization density in position space

In this appendix, we explain why the Dirac-delta contribution was missed in the calculation of the vacuum-polarization density in position space in Appendix D of Ref. 30. The error was to conclude from the expression of the vacuum-polarization density matrix in position space in Eq. (D10) of Ref. 30,

$$\mathbf{n}_1^{\text{VP}}(x, x') = \frac{1}{2\pi} \int_{-\infty}^{\infty} \Delta \mathbf{G}(x, x'; iu) du \quad (\text{C1})$$

where $\Delta \mathbf{G}(x, x'; iu)$ is the variation of the position-space Green function, that the position-space vacuum-polarization density was given by the expression in Eq. (D11) of Ref. 30,

$${}^{\prime\prime}n^{\text{VP}}(x) = \frac{1}{2\pi} \int_{-\infty}^{\infty} \text{tr}[\Delta \mathbf{G}(x, x; iu)] du. \quad (\text{C2})$$

Indeed, while $\Delta \mathbf{G}(x, x'; iu)$ is continuous around the diagonal $x = x'$ for a given u , the integral over u contains a singular contribution which is not continuous at $x = x' = 0$. This singular term in $\text{tr}[\mathbf{n}_1^{\text{VP}}(x, x')]$, at first order in Z for simplicity, is

$$\begin{aligned} \text{tr}[\mathbf{n}_{1, \text{sing}}^{\text{VP}, (1)}(x, x')] &= -\frac{Z}{4\pi c^2} [\text{sgn}(x) \text{sgn}(x') - 1] \int_{-\infty}^{\infty} e^{-\kappa(iu)(|x| + |x'|)} du \\ &= -\frac{mZ}{2\pi} [\text{sgn}(x) \text{sgn}(x') - 1] K_1(mc(|x| + |x'|)), \end{aligned} \quad (\text{C3})$$

where K_1 is the modified Bessel function of the second kind. This term has a diagonal $x = x'$ that vanishes for $x \neq 0$, but gives raise of the Dirac-delta contribution in the Uehling vacuum-polarization density $n^{\text{VP}, (1)}(x)$. To see this, we first use $K_1(z) \sim 1/z$ as $z \rightarrow 0$ to find

$$\text{tr}[\mathbf{n}_{1, \text{sing}}^{\text{VP}, (1)}(x, x')] \underset{x, x' \rightarrow 0}{\sim} \frac{Z}{2\pi c} \frac{[1 - \text{sgn}(x) \text{sgn}(x')]}{|x| + |x'|}. \quad (\text{C4})$$

In the spirit of Refs. 99 and 100, we define the $x = x'$ diagonal of the kernel $\text{tr}[\mathbf{n}_{1,\text{sing}}^{\text{vp},(1)}(x, x')]$ by averaging it around the diagonal as

$$n_{\text{sing}}^{\text{vp},(1)}(x) = \lim_{\epsilon \rightarrow 0^+} \frac{1}{(2\epsilon)^2} \int_{x-\epsilon}^{x+\epsilon} \int_{x-\epsilon}^{x+\epsilon} \text{tr}[\mathbf{n}_{1,\text{sing}}^{\text{vp},(1)}(y, y')] dy dy'. \quad (\text{C5})$$

This gives

$$n_{\text{sing}}^{\text{vp},(1)}(x) = \frac{Z}{\pi c} \lim_{\epsilon \rightarrow 0^+} \frac{f(x/\epsilon)}{\epsilon}, \quad (\text{C6})$$

where

$$f(x) = \begin{cases} (1/2) \ln(4/(1-x^2)) - x \operatorname{arctanh}(x), & |x| < 1 \\ 0, & |x| \geq 1, \end{cases} \quad (\text{C7})$$

and $\int_{-\infty}^{\infty} f(x) dx = 1$. Thus, in the sense of distributions, the limit in Eq. (C6) tends to a Dirac-delta function

$$n_{\text{sing}}^{\text{vp},(1)}(x) = \frac{Z}{\pi c} \delta(x), \quad (\text{C8})$$

in agreement with Eq. (32). The derivation in momentum space presented in Section II B of this paper is valid without the need of a regularization like in Eq. (C5), because $\text{tr}[\hat{\mathbf{n}}_1^{\text{vp},(1)}(p, p')]$ is smooth in (p, p') .

Appendix D: Rate of convergence of the bound-state energy in a plane-wave basis

In this appendix, we study the rate of convergence of the bound-state energy of the 1D hydrogen-like Dirac atom in a plane-wave basis.

The exact bound-state eigenfunction of the 1D hydrogen-like Dirac Hamiltonian \mathbf{D}_Z has the form (see Eq. (8))

$$\boldsymbol{\psi}_b^Z(x) = \begin{pmatrix} \psi^L(x) \\ \psi^S(x) \end{pmatrix}, \quad (\text{D1})$$

with $\psi^L(x) = A_b e^{-\kappa_b |x|}$ and $\psi^S(x) = A_b i \operatorname{sgn}(x) (Z/2c) e^{-\kappa_b |x|}$ (the expressions of the constants A_b and κ_b are given after Eq. (8)). The associated exact bound-state energy is

$$\begin{aligned} \varepsilon_b^Z &= \langle \boldsymbol{\psi}_b^Z, \mathbf{D}_Z \boldsymbol{\psi}_b^Z \rangle \\ &= \langle \boldsymbol{\psi}_b^Z, mc^2 \boldsymbol{\sigma}_3 \boldsymbol{\psi}_b^Z \rangle. \end{aligned} \quad (\text{D2})$$

The last equality in Eq. (D2) comes from the relativistic virial theorem [101–103], which can be shown, e.g. using a scaling argument, to have the same form for the 1D Dirac equation with a Dirac-delta potential as for the 3D Dirac equation with a Coulomb potential. It provides a convenient expression for calculating the energy.

We consider a complete plane-wave basis $\{\chi_n\}_{n \in \mathbb{Z}}$ on the interval $[-L/2, L/2]$ where $\chi_n(x) = (1/\sqrt{L}) e^{ik_n x}$ and $k_n = 2\pi n/L$, and use it to expand the restriction of the exact bound-state eigenfunction $\boldsymbol{\psi}_b^Z$ to the interval $[-L/2, L/2]$. Since ψ^L and ψ^S are even and odd functions, respectively, we introduce even and odd basis functions

$$\chi_n^g(x) = \begin{cases} \chi_0(x) & \text{for } n = 0 \\ \frac{\chi_n(x) + \chi_{-n}(x)}{\sqrt{2}} & \text{for } n \in \mathbb{N}^* \end{cases} \quad \text{and} \quad \chi_n^u(x) = \frac{\chi_n(x) - \chi_{-n}(x)}{\sqrt{2}} \quad \text{for } n \in \mathbb{N}^*. \quad (\text{D3})$$

For $x \in [-L/2, L/2]$, we have thus

$$\psi^L(x) = \sum_{n=0}^{\infty} c_n^L \chi_n^g(x) \quad \text{and} \quad \psi^S(x) = \sum_{n=1}^{\infty} c_n^S \chi_n^u(x), \quad (\text{D4})$$

with coefficients

$$c_n^L = \langle \psi^L, \chi_n^g \rangle_L = \begin{cases} \frac{2A_b}{\kappa_b \sqrt{L}} (1 - e^{-\kappa_b L/2}) & \text{for } n = 0 \\ \frac{2\sqrt{2}A_b \kappa_b}{\sqrt{L}} \frac{1 - (-1)^n e^{-\kappa_b L/2}}{\kappa_b + k_n^2} & \text{for } n \in \mathbb{N}^* \end{cases} \quad \text{and} \quad c_n^S = \langle \psi^S, \chi_n^u \rangle_L = -\frac{Zk_n}{2c\kappa_b} c_n^L \quad \text{for } n \in \mathbb{N}^*. \quad (\text{D5})$$

As $n \rightarrow \infty$, the large-component coefficients c_n^L decay as $1/n^2$ while the small-component coefficients c_n^S decay as $1/n$.

We now consider the best approximation (in the sense of the L^2 norm) $\tilde{\psi}_b^Z$ to ψ_b^Z in the finite basis $\{\chi_n\}_{|n| \leq n_{\max}}$, for $x \in [-L/2, L/2]$,

$$\tilde{\psi}_b^Z(x) = \begin{pmatrix} \tilde{\psi}_b^L(x) \\ \tilde{\psi}_b^S(x) \end{pmatrix}, \quad (\text{D6})$$

where

$$\tilde{\psi}_b^L(x) = \sum_{n=0}^{n_{\max}} c_n^L \chi_n^g(x) \quad \text{and} \quad \tilde{\psi}_b^S(x) = \sum_{n=1}^{n_{\max}} c_n^S \chi_n^u(x). \quad (\text{D7})$$

The corresponding approximation to the bound-state energy, as a function of the IR cutoff L and the UV cutoff $\Lambda = 2\pi n_{\max}/L$, is

$$\tilde{\varepsilon}_b^Z(L, \Lambda) = \langle \tilde{\psi}_b^Z, mc^2 \boldsymbol{\sigma}_3 \tilde{\psi}_b^Z \rangle_L = mc^2 \left(\sum_{n=0}^{n_{\max}} |c_n^L|^2 - \sum_{n=1}^{n_{\max}} |c_n^S|^2 \right). \quad (\text{D8})$$

From the expression of the coefficients in Eq. (D5), we find the behavior of the bound-state energy as $\Lambda \rightarrow \infty$

$$\tilde{\varepsilon}_b^Z(L, \Lambda) \underset{\Lambda \rightarrow \infty}{\sim} \tilde{\varepsilon}_b^Z(L, \infty) + \frac{A_b^2 Z^2 (1 + e^{-\kappa_b L})}{\pi c^2 \Lambda}, \quad (\text{D9})$$

with

$$\tilde{\varepsilon}_b^Z(L, \infty) = \lim_{\Lambda \rightarrow \infty} \tilde{\varepsilon}_b^Z(L, \Lambda) = (1 - e^{-\kappa_b L}) \varepsilon_b^Z, \quad (\text{D10})$$

where ε_b^Z is the exact bound-state energy. We thus find that $\tilde{\varepsilon}_b^Z(L, \Lambda)$ converges as $1/\Lambda$ as $\Lambda \rightarrow \infty$. This asymptotic convergence rate comes entirely from the small-component contribution which, having a discontinuity at $x = 0$ in addition to a derivative discontinuity, represents the limiting factor in the convergence of the bound-state energy. We also see that, at least for large enough Λ , the bound-state energy converges exponentially with L as $L \rightarrow \infty$. Even though the best approximate eigenfunction $\tilde{\psi}_b^Z$ in the sense of the L^2 norm considered here does not exactly correspond to the approximate eigenfunction obtained in Section III A by diagonalizing the Hamiltonian in the plane-wave basis, in practice we expect a similar convergence rate for the latter case.

ACKNOWLEDGEMENTS

U.M. has received funding from the European Union's Horizon 2020 research and innovation programme under the Marie Skłodowska-Curie grant agreement N°945332.

-
- [1] P. Pyykkö, *Annu. Rev. Phys. Chem.* **63**, 45 (2012).
 - [2] P. Pyykkö, *Chem. Rev.* **112**, 371 (2012).
 - [3] J. Autschbach, *J. Chem. Phys.* **136**, 150902 (2012).
 - [4] T. Saue and L. Visscher, in *Theoretical Chemistry and Physics of Heavy and Superheavy Elements*, edited by S. Wilson and U. Kaldor (Kluwer, Dordrecht, 2003), pp. 211–267.
 - [5] K. G. Dyall and K. Fægri, Jr., *Introduction to Relativistic Quantum Chemistry* (Oxford University Press, 2007).
 - [6] M. Reiher and A. Wolf, *Relativistic Quantum Chemistry: The Fundamental Theory of Molecular Science* (WILEY-VCH, Weinheim, 2009).
 - [7] P. J. Mohr, G. Plunien and G. Stoff, *Phys. Rep.* **293**, 227 (1998).
 - [8] V. M. Shabaev, *Phys. Rep.* **356**, 119 (2002).
 - [9] I. Lindgren, S. Salomonson and B. Asén, *Phys. Rep.* **389**, 162 (2004).
 - [10] P. Indelicato and P. J. Mohr, in *Handbook of Relativistic Quantum Chemistry*, edited by W. Liu (Springer, Berlin, Heidelberg, 2017), pp. 131–241.
 - [11] A. Nonn, A. Margócsy and E. Mátyus, *J. Chem. Theory Comput.* (2024).
 - [12] P. Pyykkö and L.-B. Zhao, *J. Phys. B* **36**, 1469 (2003).
 - [13] V. M. Shabaev, I. I. Tupitsyn and V. A. Yerokhin, *Phys. Rev. A* **88**, 012513 (2013).

- [14] P. Schwerdtfeger, L. F. Pašteka, A. Punnett and P. O. Bowman, Nucl. Phys. A **944**, 551 (2015).
- [15] L. F. Pasteka, E. Eliav, A. Borschevsky, U. Kaldor and P. Schwerdtfeger, Phys. Rev. Lett. **118**, 023002 (2017).
- [16] A. V. Malyshev, D. A. Glazov, V. M. Shabaev, I. I. Tupitsyn, V. A. Yerokhin and V. A. Zaytsev, Phys. Rev. A. **106**, 012806 (2022).
- [17] M. Salman, *Corrections électrodynamiques quantiques en chimie quantique*, Ph.D. thesis, Université Paul Sabatier (2022).
- [18] L. V. Skripnikov, J. Chem. Phys. **154**, 201101 (2021).
- [19] A. Sunaga, M. Salman and T. Saue, J. Chem. Phys. **157**, 164101 (2022).
- [20] D. J. Flynn, H. M. Quiney and I. P. Grant, arXiv:2405.11262 (2024).
- [21] D. J. Flynn, H. M. Quiney and I. P. Grant, arXiv:2405.11261 (2024).
- [22] P. Chaix and D. Iracane, J. Phys. B **22**, 3791 (1989).
- [23] W. Kutzelnigg, Chem. Phys. **395**, 16 (2012).
- [24] W. Liu and I. Lindgren, J. Chem. Phys. **139**, 014108 (2013).
- [25] W. Liu, Phys. Rep. **537**, 59 (2014).
- [26] W. Liu, Int. J. Quantum Chem. **115**, 631 (2015).
- [27] W. Liu, J. Chem. Phys. **152**, 180901 (2020).
- [28] J. Toulouse, SciPost Chem. **1**, 002 (2021).
- [29] W. Liu, WIREs Comput. Mol. Sci. p. e1652 (2022).
- [30] T. Audinet and J. Toulouse, J. Chem. Phys. **158**, 244108 (2023).
- [31] C. Hainzl, M. Lewin and E. Séré, Commun. Math. Phys. **257**, 515 (2005).
- [32] C. Hainzl, M. Lewin and E. Séré, J. Phys. A **38**, 4483 (2005).
- [33] C. Hainzl, M. Lewin and J. P. Solovej, Comm. Pure Appl. Math. **60**, 0546 (2007).
- [34] C. Hainzl, M. Lewin, E. Séré and J. P. Solovej, Phys. Rev. A **76**, 052104 (2007).
- [35] P. Gravejat, M. Lewin and E. Séré, Commun. Math. Phys. **286**, 179 (2009).
- [36] C. Hainzl, M. Lewin and E. Séré, Arch. Rational Mech. Anal. **192**, 453 (2009).
- [37] P. Gravejat, M. Lewin and E. Séré, Commun. Math. Phys. **306**, 1 (2011).
- [38] M. Lewin, in *Mathematical Results In Quantum Physics: Proceedings of the Qmath11 Conference*, edited by P. Exner (World Scientific Publishing, 2011), pp. 45–59.
- [39] M. Rodriguez-Mayorga, K. J. H. Giesbertz and L. Visscher, SciPost Chem. **1**, 004 (2021).
- [40] C. Hainzl and H. Siedentop, Commun. Math. Phys. **243**, 241 (2003).
- [41] A. A. Frost, J. Chem. Phys. **25**, 1150 (1956).
- [42] D. R. Herrick and F. H. Stillinger, Phys. Rev. A **11**, 42 (1975).
- [43] D. R. Herschbach, J. Chem. Phys. **84**, 838 (1986).
- [44] D. Traore, E. Giner and J. Toulouse, J. Chem. Phys. **156**, 044113 (2022).
- [45] R. Subramanian and K. V. Bhagwat, J. Phys. C **5**, 798 (1972).
- [46] I. R. Lapidus, Am. J. Phys. **51**, 1036 (1983).
- [47] F. Fillion-Gourdeau, E. Lorin and A. D. Bandrauk, J. Phys. A **45**, 215304 (2012).
- [48] J. M. Guilarte, J. M. Muñoz-Castaneda, I. Pirozhenko and L. Santamaria-Sanz, Frontiers in Physics **7**, 109 (2019).
- [49] Y. Nogami and D. J. Beachey, Europhys. Lett. **2**, 661 (1986).
- [50] P. Šeba, Lett. Math. Phys. **18**, 77 (1989).
- [51] S. Benvegnù and L. Dabrowski, Lett. Math. Phys. **30**, 159 (1994).
- [52] R. J. Hughes, Rep. Math. Phys. **39**, 425 (1997).
- [53] R. J. Hughes, J. Math. Anal. Appl. **238**, 67 (1999).
- [54] K. Pankrashkin and S. Richard, J. Math. Phys. **55**, 062305 (2014).
- [55] F. A. B. Coutinho and Y. Nogami, Phys. Rev. A. **36**, 1008 (1987).
- [56] M. Loewe and M. Sanhueza, J. Phys. A **23**, 553 (1990).
- [57] Y. Nogami, N. P. Parent and F. M. Toyama, J. Phys. A **23**, 5667 (1990).
- [58] E. H. Wichmann and N. M. Kroll, Phys. Rev. **101**, 843 (1956).
- [59] C. Hainzl, Ann. Henri Poincaré **5**, 1137 (2004).
- [60] M. J. Esteban, M. Lewin and E. Séré, Bull. Amer. Math. Soc. **45**, 535 (2008).
- [61] J. J. Sakurai, *Advances Quantum Mechanics* (Addison-Wesley, 1967).
- [62] W. Greiner and J. Reinhardt, *Quantum Electrodynamics, 4th edition* (Springer-Verlag, Berlin Heidelberg, 2009).
- [63] An equivalent alternative expression of $\mathbf{n}_{\text{reg}}^{\text{vp}}(x)$ was also given in Eq. (66) of Ref. [30]. In the latter equation, a $\text{sgn}(x)$ function was missing in the off-diagonal elements of $\mathbf{n}_{\text{reg}}^{\text{vp}}(x)$.
- [64] J. Goldstone and F. Wilczek, Phys. Rev. Lett. **47**, 986 (1981).
- [65] A. J. Niemi and G. W. Semenoff, Phys. Rep. **135**, 99 (1986).
- [66] I. V. Krive and A. S. Rozhavskii, Sov. Phys. Usp. **30**, 370 (1987).
- [67] K. Rao, N. Sahu and P. Panigrahi, Reson. **13**, 738 (2008).
- [68] S. Kivelson and J. R. Schrieffer, Phys. Rev. B **25**, 6447 (1982).
- [69] R. Rajaraman and J. S. Bell, Phys. Lett. **116B**, 151 (1982).
- [70] Y. Nogami, arXiv:0808.0164 (2008).
- [71] R. Jackiw and C. Rebbi, Phys. Rev. D **13**, 3398 (1976).
- [72] D. Shale and W. F. Stinespring, J. Math. Mech. **14**, 315 (1965).
- [73] B. Thaller, *The Dirac Equation* (Springer-Verlag, Berlin, Heidelberg, 1992).
- [74] P. Falkensteiner and H. Grosse, Lett. Math. Phys. **14**, 139 (1987).

- [75] H. Grosse and G. Opelt, Nucl. Phys. B **285**, 143 (1987).
- [76] M. Salman and T. Saue, Phys. Rev. A. **108**, 012808 (2023).
- [77] M. I. Eides, H. Grotch and V. A. Shelyuto, Phys. Rep. **342**, 63 (2001).
- [78] R. E. Stanton and S. Havriliak, J. Chem. Phys. **81**, 1910 (1984).
- [79] W. Kutzelnigg, Int. J. Quantum Chem. **25**, 107 (1984).
- [80] V. M. Shabaev, I. I. Tupitsyn, V. A. Yerokhin, G. Plunien and G. Soff, Phys. Rev. Lett. **93**, 130405 (2004).
- [81] Q. Sun, W. Liu and W. Kutzelnigg, Theor. Chem. Acc. **129**, 423 (2011).
- [82] M. Salman and T. Saue, Symmetry **12**, 1121 (2020).
- [83] I. Grant and H. Quiney, Atoms **10**, 108 (2022).
- [84] M. Lewin and E. Séré, Proc. London Math. Soc. **100**, 864 (2009).
- [85] M. Lewin and E. Séré, in *Many-Electron Approaches in Physics, Chemistry and Mathematics*, edited by V. Bach and L. Delle Site (Springer International Publishing, 2014), pp. 31–52.
- [86] J.-F. Colombeau, *Multiplication of Distributions: A tool in mathematics, numerical engineering and theoretical physics* (Springer-Verlag, Berlin Heidelberg, 1992).
- [87] M. Grosser, M. Kunzinger, M. Oberguggenberger and R. Steinbauer, *Geometric Theory of Generalized Functions with Applications to General Relativity* (Springer Science+Business Media, Dordrecht, 2001).
- [88] A. Gsponer, Eur. J. Phys. **30**, 109 (2009).
- [89] P. Kurasov and J. Boman, Proc. Am. Math. Soc. **126**, 1673 (1998).
- [90] M. G. Calkin, D. Kiang and Y. Nogami, Am. J. Phys. **55**, 737 (1987).
- [91] B. H. J. McKellar and G. J. Stephenson, Jr., Phys. Rev. C **35**, 2262 (1987).
- [92] V. Alonso and S. De Vincenzo, Int. J. Theor. Phys. **39**, 1483 (2000).
- [93] B. H. J. McKellar and G. J. Stephenson, Jr., Phys. Rev. A **36**, 2566 (1987).
- [94] R. J. Hughes, Lett. Math. Phys. **34**, 395 (1995).
- [95] M. Tušek, Lett. Math. Phys. **110**, 2585 (2020).
- [96] B. Sutherland and D. C. Mattis, Phys. Rev. A. **24**, 1194 (1981).
- [97] M. G. Calkin, D. Kiang and Y. Nogami, Phys. Rev. C **38**, 1076 (1988).
- [98] L. Heriban and M. Tušek, J. Math. Anal. Appl. **516**, 126536 (2022).
- [99] C. Brislawn, Proc. Am. Math. Soc. **104**, 1181 (1988).
- [100] C. Brislawn, Pac. J. Math. **150**, 229 (1991).
- [101] M. Brack, Phys. Rev. D **27**, 1950 (1983).
- [102] V. M. Shabaev, in *Lecture Notes in Physics* (Springer Berlin Heidelberg, 2003), pp. 97–113.
- [103] C. Froese Fischer and M. Godefroid, Atoms **10**, 110 (2022).